Assessing risk for butterflies in the context of climate change, demographic uncertainty, and heterogenous data sources

Matthew L. Forister[1], Eliza M. Grames[1], Christopher A. Halsch[1], Kevin J. Burls[2], Cas F. Carroll[1], Katherine L. Bell[1], Joshua P. Jahner[3], Taylor Bradford[1], Jing Zhang[4], Qian Cong[5], Nick V. Grishin[4,6], Jeffrey Glassberg[7,8], Arthur M. Shapiro[9], Thomas V. Riecke[10]

[1] Ecology, Evolution. and Cons. Biology, Dept. of Biology, Univ. of Nevada, Reno, Nevada, USA

[2] Xerces Society for Invertebrate Conservation, Portland, Oregon, USA

[3] Department of Botany, University of Wyoming, Laramie, Wyoming, USA

[4] Howard Hughes Medical Inst., Univ. of Texas Southwest Medical Center, Dallas, Texas, USA

[5] Inst. for Protein Design and Dept. of Bioch., Univ. of Washington, Seattle, Washington, USA

[6] Depts. of Biophysics and Biochemistry, Univ. of Texas Southwest Medical Center, Dallas, Texas, USA

[7] North American Butterfly Association, Morristown, New Jersey, USA

[8] Department of BioSciences, Rice University, Houston, Texas, USA

[9] Center for Population Biology, University of California, Davis, California, USA

[10] Swiss Ornithological Institute, CH-6204 Sempach, Switzerland

Correspondence: Matthew L. Forister, mforister@unr.edu

Open Research Statement: NABA data analyzed for this paper are available at 10.5281/zenodo.4460647; Shapiro transect data and all code will be archived on figshare.com upon acceptance for publication; code used is not novel to this project (relevant functions and packages are cited).

Abstract Ongoing declines in insect populations have led to substantial concern and calls for conservation action. However, even for relatively well-studied groups, like butterflies, information relevant to species-specific status and risk is scattered across field guides, the scientific literature, and agency reports. Consequently, attention and resources have been spent on a miniscule fraction of insect diversity, including a few well-studied butterflies. Here we bring together heterogenous sources of information for 396 butterfly species to provide the first regional assessment of butterflies for the 11 western US states. For 184 species, we use monitoring data to characterize historical and projected trends in population abundance. For another 212 species (for which monitoring data are not available, but other types of information can be collected), we use exposure to climate change, development, geographic range, host breadth and other factors to rank species for conservation concern. A phylogenetic signal is apparent, with concentrations of declining and at-risk species in the families Lycaenidae and Hesperiidae. A geographic bias exists in that many species that lack monitoring data occur in more southern states where we expect that impacts of warming and drying trends will be most severe. Legal protection is relatively uncommon among the taxa with the highest risk values: of the top 100 species, one is listed as threatened under the US Endangered Species Act and one is a candidate for listing. Among the many taxa not currently protected, we highlight a short list of species in decline, including *Vanessa annabella*, *Thorybes mexicanus*, *Euchloe ausonides*, and *Pholisora catullus*. Notably, many of these species have broad geographic ranges, which perhaps highlights a new era of insect conservation in which small or fragmented ranges will not be the only red flags that attract conservation attention.

KEYWORDS Anthropocene, butterfly, climate change, Lepidoptera, population viability analysis, demographic uncertainty, extinction, heterogeneous data, hierarchical Bayesian model

INTRODUCTION

Reductions in abundance, contractions in geographic range, extirpation, and extinction have become common features of wild plant and animal populations impacted by the various stressors of the Anthropocene (Dirzo et al. 2014, Turvey and Crees 2019). Effects on individual populations translate into depauperate assemblages of species in remaining natural lands, even those far removed from the most immediate effects of habitat destruction and degradation (McLaughlin et al. 2002, Brook et al. 2008). To the extent that the loss of evolutionary lineages (populations, species and higher taxonomic groups) is a part of life on earth and always has been, the current mass extinction crisis affords ecologists the chance to study extinction as an important earth-system process (Benton 2003). However, the need to maintain functioning natural ecosystems is increasingly generating motivation among scientists and the general public to reverse or slow whatever biotic losses might still be addressed (Naeem et al. 2016). Concern for functioning ecosystems has been elevated in recent years by a steady pulse of papers reporting declines in insect abundance and diversity (Eisenhauer et al. 2019, Wagner 2019, Wepprich et al. 2019, van Klink et al. 2020) that have inspired calls for new conservation attention focused on "the little things that run the world" (Wilson 1987, Goulson 2019, Cardoso et al. 2020).

Effective conservation and management depends on the synthesis of multiple lines of information including population monitoring, natural history studies, and geographic surveys. For insects, the taxonomic diversity is so great and the available information is so sparse (Cardoso et al. 2011), that proactive conservation informed by diverse data types has rarely been an option. As a consequence, insect conservation has often been motivated largely by fragmentation and small geographic ranges (Samways 2007, Diniz-Filho et al. 2010). Exceptions

to that pattern include a few European countries where studies of butterflies have been sufficiently thorough in terms of natural history and monitoring that researchers have been able to prioritize species for conservation attention in a way that follows the International Union for Conservation of Nature (IUCN) and the Red List framework (Fox et al. 2011, van Swaay et al. 2011, Maes et al. 2012, Bonelli et al. 2018). That depth of species-specific information for insects is unusual, even for butterflies, and most countries will have a more complex mix of some monitoring or observational data, natural history observations, and expert opinion (New et al. 1995, Edge and Mecenero 2015, Geyle et al. 2021).

Butterflies in the western United States provide an excellent case study for the challenge of conservation prioritization that involves a mixture of heterogenous data types and sources of information. The region does include butterfly monitoring programs, but also expansive areas that are sparsely populated and understudied, including in particular the Intermountain West with hundreds of mountain ranges in the nearly 500k square kilometers of the Great Basin Desert. The most temporally-intensive butterfly monitoring program in the western US is the Shapiro transect of ten permanent sites across Northern California that have been monitored biweekly during the flight season for between 35 and 51 years (Shapiro 2022). Many years before the entomological world made a collective pivot to the problem of insect declines (Dirzo et al. 2014, Hallmann et al. 2017), work with the Shapiro data documented shifting spring phenologies (Forister and Shapiro 2003), and the influence of land use and warming temperatures on extensive declines in abundance and species richness (Forister et al. 2010, Casner et al. 2014b). More recently, patterns from the temporally-intensive Shapiro dataset were analyzed in parallel with geographically-extensive monitoring data from the North American Butterfly Association (NABA) and iNaturalist observations across the 11 western states (Forister et al. 2021). That

effort quantified a compounding loss of 1.6% fewer butterflies observed per year, consistent with rates of loss from other studies (Wepprich et al. 2019, van Klink et al. 2020), and highlighted the negative influence of warming and drying conditions on butterfly populations in natural areas. However, the species included in Forister et al. (2021) were only those common and widespread enough to be present with sufficient frequency in monitoring databases to allow for inclusion in statistical models. Moreover, an attempt was not made to combine different lines of information into a ranking of species for conservation concern.

Here we address that need by taking a multi-faceted approach to conservation prioritization that utilizes observational data when available (for approximately half the species) and a combination of data types for other species, including natural history traits and quantitative estimates of exposure to climate change and development. We refer to these two groups of species, with and without monitoring data, as the "A group" and "B group" species, respectively. These two groups are treated throughout this paper in distinct but complementary ways, with the dual goal of presenting a unified picture of risk for a regional butterfly fauna, but also with the objective of providing a case study for how species with different amounts of information can be mutually informative when considered together in a conservation context. The different data types studied for both A and B group species are detailed below and are used (1) to produce a quantitative ranking that highlights the taxa most severely declining and most likely to face regional extirpation or extinction in coming decades; and (2) to identify geographic and taxonomic knowledge gaps in our understanding of western butterflies. It is our hope that these results will be used by conservation practitioners and land managers to guide restoration and protection efforts, and will also motivate additional monitoring and the development of new population models that take maximum advantage of heterogenous data types. Throughout this

paper, we use the word "risk" (and related terms, like "risk index") in a flexible way that encompasses evidence of past decline, projected declines, and combinations of traits that could predispose species to ongoing and future declines. This flexibility is necessary given the nature of our project encompassing species for which different kinds and quantities of information are available, but in all cases we intend the concept of high risk to flag species that could profitably receive careful attention from ecologists, conservation biologists, and the general public.

MATERIALS AND METHODS

A schematic overview of our methods is shown in Figure 1, emphasizing the flow of information from external data sources through analyses to the generation of quantitative risk assessment. All parts of the process are discussed in detail here. The order of the sections below follows the order of variables (salmon colored boxes) in Figure 1, from left to right, starting with the process that generates P(extirpation) from the NABA data and ending with wing span and host range. After the creation of variables, the subsequent methods sections roughly correspond to the main products (green boxes) in Figure 1, from the creation of ranked lists to risk maps and the visualization of phylogenetic risk.

Starting with the 875 taxa on the North American Butterfly Association's 2nd edition checklist of butterflies occurring north of Mexico (NABA 2018), we retained 396 species with resident (non-vagrant) status in the eleven western states (Washington, Oregon, California, Idaho, Montana, Nevada, Wyoming, Colorado, Utah, New Mexico, and Arizona) based on range maps in Glassberg (2017), and collapsed 18 subspecies from that list into full species. For clarity and in order to facilitate wide use of our results, we also reference a second checklist by Pelham (2022) in places where names differ.

Of the 396 species from the NABA list, 184 were present in monitoring databases (either the Shapiro transect or the NABA count circles) with sufficient frequency to be used in population models. For those species (the A group), our approach is to rank species based on observed and forecast population trajectories. Acknowledging the great uncertainty inherent to insect time series analyses, we present the ranking of A group species in a way that risk associated with other variables (e.g., geographic range size) can be evaluated by the reader.

For the 212 species in the B group (not present in monitoring schemes in sufficient frequency for inclusion in core population models), we have accumulated seven variables that form a composite picture of risk: geographic range, exposure to developed land, exposure to climate change, average (range-wide) precipitation, voltinism (number of generations per year), wingspan, and host breadth (or "host range"). We combine those seven variables into a single risk index as a weighted sum, where the weights are determined in part by our previous work with western butterflies, but also by analyses of the A group (described in detail below). The weighting scheme and other steps in data processing involve informed but partly subjective judgments (see section below on *Calculation of risk index for A and B group species*) with respect to threats to butterflies and natural history traits that predispose butterflies to risk. We have presented all data decisions in a transparent way, so that the reader can judge for themselves the consequences of our methods and decisions, and alternative weights can be assigned by researchers using an online tool (see Supplementary Material). In the sections below, we describe first the observational datasets (NABA and Shapiro) and associated analyses, then the seven other variables and how they are combined into composite risk indices and are visualized geographically and in a phylogenetic context.

Variable creation part 1: North American Butterfly Association (NABA) counts and models

The NABA butterfly count program is a suite of hundreds of individual locations throughout the country that are monitored during midsummer (typically once, but in some cases more than once) by a group of at least four observers recording counts of all individual butterflies seen and identified to species, in a 15-mile (24.14 km) diameter circle. Observations from count circles in the 11 western states encompass different numbers of years at different sites from the 1970s to the present, with the final year in the dataset we examined being 2018 (the data were compiled for analysis in 2019). For the current project, we filtered the observations so that we only included sites that had been monitored for at least ten years, and with the final year being 2017 or 2018 (we did this so as not to generate forecasts for species with a substantial recent gap in observations). More than one monitoring day has been reported per year at a small number of sites, and for those locations we retained only the survey closest to the 4th of July, which is the traditional target date for these censuses. We then excluded any site-by-species combinations in which a species was not present for at least ten years (not necessarily consecutive years). Finally, only species meeting the latter criterion for at least three locations were retained. Those filters resulted in a dataset with 162 species from 44 locations used in the core model and associated population forecasts (we experimented with less stringent filters but found that model performance suffered). For species with less data, we ran a second set of models with lower thresholds, as described after the core model below.

Previous work with the NABA data used hierarchical Bayesian linear Poisson regressions run separately for each species (Forister et al. 2021). Here we advance that approach using a single, multi-species model that shares information about heterogeneity in the observation

process across species observed at each site (Riecke et al. 2021). The components of the model (each described in turn below) include an observation sub-model, an abundance sub-model, and a forecast or simulation process that projects occupancy (the fraction of sites with non-zero presence by species) for various intervals of years in the future.

For the observational component, we modeled the counts of individual butterflies (y) using a Poisson distribution given the expected count of each species at each location during each year ($\mu_{\mathrm{t,l,s}}$), where t, l, and s identify the year, location, and species respectively:

$$y_{\mathrm{t,l,s}} \sim \mathrm{Poisson}\left(\mu_{\mathrm{t,l,s}}\right).$$

We modeled the expected count ($\mu_{\mathrm{t,l,s}}$) as a function of an abundance index ($N_{\mathrm{t,l,s}}$), year- and site-specific survey effort (β), and a year- and location-specific random effect ($\delta_{\mathrm{t,l}}$) shared among species:

$$\mu_{\mathrm{t,l,s}} = \exp(\ln(N_{\mathrm{t,l,s}}) + \beta * \mathrm{effort}_{\mathrm{t,l}} + \delta_{\mathrm{t,l}}),$$

with a vague prior for the effect of survey effort:

$$\beta \sim \mathrm{normal}(0,10).$$

The empirical variable for effort is the z-standardized total hours searched by all survey groups at a site on a day. After accounting for the effect of survey effort, we modeled additional variation in detection probability for each survey or monitoring day as a random effect shared among species. This random effect can be thought of as the combined effects of survey-specific variation in detection due to processes such as variation in observer experience and local weather conditions (Riecke et al. 2021):

$$\delta_{\mathrm{t,l}} \sim \mathrm{normal}(0, \varsigma^2),$$

$$\varsigma \sim \mathrm{gamma}(1,1).$$

For the abundance sub-model, we assigned priors for initial population abundance indices for each species at their first encounter ($f_{\mathrm{site}_i,\mathrm{species}_i}$) at a study site as a function of initial survey effort and the initial count:

$$N_{\mathrm{f_{l,s}},\mathrm{l,s}} \sim \mathrm{gamma}(\exp[\ln(y_{\mathrm{f_{l,s}},\mathrm{l,s}}) + (\mathrm{effort}_{\mathrm{f_{l,s}},\mathrm{l,s}} * -0.1)], 1).$$

We modeled changes in population size (N) from one year to the next for each species at each site as a function of year (t), location (l), and a species(s)-specific population growth rate (λ):

$$N_{t+1,l,s} = N_{t,l,s} * \lambda_{t,l,s}\ .$$

Variation in population growth rate was in turn modeled as a function of a species-specific mean population growth rate (γ_s), and species-specific random variance in population growth rate:

$$\lambda_{t,l,s} \sim \mathrm{lognormal}(\gamma_s, \sigma_s^2),$$

$$\gamma_s \sim \mathrm{normal}(0,1),$$

$$\sigma_s^2 \sim \mathrm{gamma}(1,1).$$

Finally, for each species at each location, we projected the abundance index into the future using Monte Carlo simulation from the posterior distributions of species-specific population growth rate ($\lambda_{t,l,s}$), and species-specific population growth rate variance (σ_s^2):

$$N_{t+1,l,s} = N_{t,l,s} * \lambda_{t,l,s},$$

$$\lambda_{t,l,s} \sim \mathrm{lognormal}(\gamma_s, \sigma_s^2).$$

We defined local 'extirpations' as locations at which the expected count of a species given mean effort was less than 0.1 individuals, and calculated extirpation probability for each species at 10, 20, and 50 years into the future. Thus, one minus the extirpation probability is the probability of population persistence, and it is that value (probability of persistence) for each species from the core NABA model that moves forward (represented by 1k samples from the final year of the simulations) into the calculation of the risk index for the A group species.

The above model and 50-year projections were used for 162 species (in the A group) with sufficient data (passing filters described above). For another 105 species (with a median presence of 2 sites per species), we used a less complex model. These species are part of the B group with minimal observational data that were too sparse to be included in the core NABA model described above. However, in the interest of presenting maximal information on all species, we estimated trends through time for this subset of the B group (albeit at many fewer sites per species); the results are reported but not incorporated into the risk index calculation for these species. In this model, the counts (y) were also modeled with a Poisson distribution given the expected count for each location and year ($\mu_{\mathrm{t,l}}$), where t is the year and l is the location:

$$y_{\mathrm{t,l}} \sim \mathrm{Poisson}\left(\mu_{\mathrm{t,l}}\right).$$

The expected count ($\mu_{\mathrm{t,l}}$) was then modeled as a linear function of a site-specific intercept (α_{l}), a site-specific (s) year effect (β_1), and site-specific effect of effort (β_2):

$$\ln\left(\mu_{\mathrm{t,l}}\right) = \alpha_{\mathrm{l}} + \beta_{1,\mathrm{s}} * \mathrm{year}_{\mathrm{t}} + \beta_{2,\mathrm{s}} * \mathrm{effort}_{\mathrm{t,l}}.$$

The intercept and both beta coefficients were drawn from normal priors, with the normal truncated at zero to be positive for effort (β_2); the means and variances of those distributions were in turn drawn from hyperpriors (thus estimating effects across sites) with means drawn from normal distributions (with mean of zero and variance of 100) and variances drawn from gamma(1,1) as in the core model above. For 35 species present at only a single site, the model was run without the hierarchical (across sites) structure. The output of these secondary models (for the 105 species) was retained as a directional probability (the fraction of the posterior distribution above zero for species with a positive year coefficient, and below zero for species with a negative year coefficient).

A potential issue with once-per-year sampling, as in the NABA data, is sensitivity to phenological shifts. For example, for a species with one generation per year (univoltine), it is possible that earlier spring emergence associated with a warming climate could cause a mid-summer census date to fall after a population peak, and thus appear as a population decline. On the other hand, we have found that earlier emergence for butterflies in low elevation California tends to be associated with elevated numbers throughout the summer as populations have more time for growth (Forister et al. 2018). To consider these possibilities here, we developed an alternative version of our core Bayesian model (described above) in which sampling date is included as a linear covariate with effects estimated separately for univoltine and multivoltine species. Results from that model were nearly indistinguishable from results from our primary model (see Figure S1 for this and other relevant results), thus in the interest of parsimony we do not include the phenological term in our core model and results presented throughout the rest of this paper. We also used a subset of years from the Shapiro data in which count data are available to simulate the NABA monitoring scheme (with a single, variable summer date), and we asked if species that have shifted to an earlier emergence over time would appear as species in decline. Consistent with previous work (Forister et al. 2018), earlier emergence tends to be associated with stable or increasing populations, and univoltine species do not appear as outliers in that relationship (Figure S2); moreover, inferences about changes in population density over time are similar in once-per-year sampling and the full data with many visits per year (Figure S2). The role of phenological change in population response to anthropogenic stressors, including climate change, remains an important issue, but does not bias the results presented here.

All Bayesian models were implemented using JAGS (version 4.3) and the `jagsUI` package (Kellner 2017) in R (R Core Team 2020). The core model (for A group species) was run with three chains for 500k iterations, with a 250k iteration burn-in. The secondary models (for the 105 B group species with some presence in the NABA data) were run with two chains for 2k steps and a 1k burn-in. Model diagnostics included inspection of plots of chain histories (all chains converged; $\hat{R} < 1.01$), and effective samples sizes.

Variable creation part 2: Shapiro transect data and models

Ten long-term study sites across northern California have been monitored for between 35 and 51 years (depending on the site), with the presence of all butterflies noted along fixed routes every two weeks during the flight season. Data used here were compiled in 2021, including observations through 2020; earlier years were truncated so the dataset starts at 1985, except for three sites where data collection began in 1988. Species by site combinations of at least eight years were retained for analyses of 133 species. Additional details on sites, butterflies and field methods have been described elsewhere (Forister et al. 2010, Halsch et al. 2021, Shapiro 2022). In brief, data from the Shapiro sites have been analyzed using hierarchical Bayesian linear models in which the response variable (the number of days a species is observed in a year) is modeled as a binomial process, with a beta coefficient from the year term in the linear model representing change through time in the probability that a species is observed (Nice et al. 2014, Halsch et al. 2021). Here we use the version of this model and implementation as described in Forister et al. (2021) in which the model was run separately for each species and beta coefficients for years are estimated within and across sites; the higher level coefficients (across sites) are used as indices of population change for each species across the northern California

sites. As with the NABA models, model diagnostics included inspection of convergence and effective sample sizes. For downstream analyses (the creation of the risk index for A group species), 1k samples were retained from the posterior distributions of the year coefficients estimated across sites for each species. For two species, *Lycaena rubidus* and *Agraulis vanillae*, the year coefficients were extreme outliers (in the negative and positive direction, respectively) and were not used in the creation of the risk index values (described below) but we do include those coefficients in visual summaries of patterns across species.

The year coefficients from this modeling approach have been shown to be effective indices of change in total abundance as reflected in total counts of individuals which are available from a subset of years and sites (Casner et al. 2014a). Unlike the main NABA model, described in the previous section, we have not taken a forecasting approach with the Shapiro data. The two datasets have different strengths and weaknesses. The strengths of the Shapiro data are intensity and consistency of observation, which lend precision to estimates of species-specific change through time. In contrast, the NABA observations are only once per year, but because they are counts of individuals for all years they can be used to estimate population growth rates (see model description above) which can in turn be used to forecast population occupancy.

Variable creation parts 3 and 4: Geographic ranges and voltinism

Expert-derived range estimates from Glassberg (2017, 2018) were generated from Keyhole Markup Language (.kml) files for each species. The range of each species was separated by voltinism (the number of generations per year in different portions of the range), with spatial polygons retained separately for uni-, bi-, and multivoltine regions. Quantitative area estimates

were then derived for each species within the US and Mexico using the area function in the R package `raster` v3.5-11(Hijmans et al. 2021), which estimates area based on the size of raster cells. For species with ranges spanning from the 48 states into Canada and Alaska, we scanned range maps from Scott (1986) and quantified those northern range portions with the software ImageJ (Collins 2007). These area estimates were added to the values derived from the other sources (Glassberg 2017, 2018). In general, area estimates become biased closer to the poles, but our use of range estimates is relative and we expect the imprecision to have little effect on results.

In addition to estimating the total area of geographic ranges, the outlines of the expert-derived ranges were used for multiple purposes, including calculating the fraction of each range that is univoltine. For simplicity, we focus on a univoltine vs bivoltine plus multivoltine comparison, rather than considering bivoltinism as a distinct category. The outlines of the expert-derived ranges were also used to calculate exposure to land use and climatic variables (as described in the next section). Note that these other lines of geographic information, from voltinism to exposure to development and climate change, are focused on the 11 states of the western US and do not consider, for example, climate change in other regions.

Variable creation parts 5 through 7: Land use, climate, and climate change

Previous work with butterflies in our region has revealed effects of land use and climate change that are complex, potentially interacting, and dependent on both the species involved and the landscape context (Casner et al. 2014b, Forister et al. 2018, Halsch et al. 2021). Summarizing exposure to land use and climate change is not a simple task, but we have taken the relatively straightforward option of using the range outline (described in previous section) to quantify these

stressors within the range of each species. Note that this differs from the use of point locations to quantify proximity to, for example, urban development (Jamwal et al. 2021). The range-outline approach is a better fit for our goals simply because all species have the same starting data (the expert-derived ranges), which would not be true of 396 species using available point-occurrence records in, for example, iNaturalist. For highly mobile animals, like butterflies, the range-outline method has another advantage in that we do not have to assume that point locations of observations represent the only or most relevant habitats.

To quantify land use change, we reclassified the 2020 Cropland Data Layer (USDA 2020) into land cover types of agriculture, development, or natural and semi-natural habitats using the associated Cropland Data Layer scheme; all crops were classified as agriculture, development of any intensity level as development, and remaining land cover types (including pastureland) as natural or semi-natural habitat. For each species, we used the spatial polygon generated from the range map to clip the rasterized land cover types and calculated the proportion that was agriculture or development. This was done separately for regions of different voltinism, but these were summed to a single value for each species (see Figure S3 for examples of range-wide exposure to land use).

To estimate climate change exposure, we used TerraClimate data for minimum temperature, maximum temperature, and precipitation (Abatzoglou et al. 2018), which we resampled from ~4km^2 spatial resolution to ~40km^2 for computational efficiency. Using multivariate Mahalanobis distance as a measure of departure (Farber and Kadmon 2003, Abatzoglou et al. 2020), we calculated departure from baseline conditions (1958-1987) for the most recent thirty years (1991-2020) for each cell. To estimate exposure to climate change, we calculated rate of change in departure over time using Theil-Sen slopes (Theil 1950, Sen 1968)

which estimate the median slope between each pairwise set of observations and are relatively robust to outliers near the start or end of a series. We generated a raster of these trends in departures for the eleven western states. For each species, we then clipped the climate departure raster layer using the species range maps as spatial polygons and calculated the mean climate change exposure across that portion of the range (as with land use, this was done separately by voltinism, but then added for a single value per species for further analyses; see Figure S3 for examples). We also calculated 30-year climate normals (1991-2020) for minimum temperature, maximum temperature, and precipitation annually and within each season across the entire range for each species. Among those three variables, precipitation was recently found to be predictive of changes in butterfly abundance across the west (Forister et al. 2021), thus it was used as a static description of climate for inclusion in the composite risk index (described below).

Variable creation parts 8 and 9: Wingspan and host range

Among the many morphological and natural history traits that could be informative of status and risk, body size and ecological specialization are widely studied, and thus relevant data are available for many species. More narrow diets are often associated with greater sensitivity to habitat loss and other disturbance (Hughes et al. 2000), and dispersal ability is a key determinant of metapopulation resilience in the face of fragmentation or other stressors. Wingspan has been shown to be a proxy for dispersal ability in butterflies (Sekar 2012). For most of the butterflies studied here, wingspan was previously estimated (in Forister et al. 2021) with data derived from Opler (1999). For a small number of species included in the present study for which a measurement was not available from that source, we supplemented with ad hoc online searches. Similarly with diet breadth (or host range), we used a single source for the vast majority of

species (Scott 1986), and supplemented from other field guides and other online resources for the few species with missing data.

We gathered both the number of plant genera and plant families reported as caterpillar hosts for each species, and then calculated a combined index of diet breadth as the number of taxonomic families plus the natural log of the number of genera. That calculation of taxonomic diet breadth puts most weight on the number of families but allows for some influence of the number of genera eaten. For example: a species that uses hosts in two genera in two families would have a diet breadth of 2.69 (2 + ln(2)), while a species that uses plants in three genera in two families would have a diet breadth of 3.10 (2 + ln(3)). We did not attempt to gather species-level host records, for which too much data would be missing or unreliable.

Products part 1a: Transformations prior to risk index calculation

In total, we compiled nine variables that contribute to the prioritization of A and B group species in different ways: (1) 50-year occupancy projections (probabilities of population persistence) based on NABA data; (2) historical rates of change from the Shapiro data; (3) geographic range based on expert assessment; (4) exposure to agricultural and other developed lands; (5) exposure to climate change; (6) average precipitation throughout the range; (7) the fraction of the range with one generation per year; (8) wingspan; and (9) an index of diet or host breadth (Figure 1). Prior to their use in assigning a risk value to each species (discussed in the next section), each variable was subjected to a specific set of transformations that resulted in a variable with a range of 0 to 1 where larger values represent greater risk. Depending on the nature of the variable (when larger values do or do not naturally represent higher risk), the transformations included a change of sign, and (for all variables) standardization between 0 and 1 (by dividing by the largest

value). In some cases, for highly skewed variables, a natural log transformation was applied as the first step, and all transformations and scaling steps are illustrated in Figure S4.

For visualization of the transformed and scaled variables and for comparison among species, we divided the distributions (Figure S4) into quantiles and assigned circles of different sizes to the different intervals, with larger circles indicating larger values and greater assumed risk. For most of the variables, we found that the following breakpoints provided a useful assignment of circles for visualization: 0.15, 0.5, and 0.85; in other words, the interval from 0 to 0.15 was assigned the smallest circle (the least risk), from 0.15 to 0.5 the next largest, etc. Breakpoints differed for some of the more skewed variables (e.g., host range), but the results are interpreted in the same way (larger circles represent larger assumed risk).

Products part 1b: Calculation of risk index for A and B group species

The A group taxa are those species for which data were available from at least one of the monitoring programs, the Shapiro transect or the NABA network of count circles. For these species, we calculated a weighted sum based on those two lines of information with weights split evenly between them: 50% NABA and 50% Shapiro. Thus, a species with the most severe declining values for each dataset would receive a composite risk score of 1. To incorporate uncertainty retained from Bayesian analyses of the NABA and Shapiro data, the composite risk index was recalculated 1k times using 1k samples of the relevant posterior distributions; we then calculated a mean and 85% highest density interval of risk for each species. Alternative weighting schemes among all variables (including the two monitoring variables) can be explored using an interactive, online tool; see Supplementary Material.

The B group species are those lacking monitoring data. Thus, we used a composite of the other seven variables to estimate risk. We experimented with a number of weighting schemes for those seven variables and settled on an approach that was partly influenced by previous research (e.g., Forister et al. 2021) but also informed by an additional analysis of the species in the monitoring data. Specifically (for that additional analysis), we took the composite risk index for the A group species (based on NABA and Shapiro data) and used a linear regression model to determine which of the other seven variables were most predictive of that risk index (following general protocols with other Bayesian models as described above). The exact weighting scheme for B group species (influenced partly by results of the analysis of the A group) is described fully in results below. Clearly many schemes are possible for a weighted sum of seven variables, and we report correlations among outcomes from different schemes. Finally, many of the B group species had some data from the NABA dataset that were not sufficient for inclusion in our main model and occupancy forecasts. For those species, we ran a less complex model (described above as the secondary set of NABA models) and report the results along with other B group results, but we do not incorporate those values into the B group risk index to maintain consistency in risk index calculations.

The calculation of the risk index for both the A and B groups relied on a complete data matrix. For most of the variables used for the B group, there were no missing values, specifically for all of the variables deriving in part from the expert geographic ranges: range area, voltinism, precipitation, development, and climate departure (Figure 1). A few species lacked data for host range, and these we filled with interpolation of the median value calculated across all species. Similarly, median interpolation was used with the observational data and the A group species. In other words, a species without sufficient NABA observations for analysis was given the median

value associated with that variable (across other species in that dataset) prior to the calculation of the risk index.

Products part 2 and 3: Geographic and Phylogenetic visualization of risk

Finally, we asked how the composite risk indices were distributed across the landscape and across the phylogeny of western butterflies. From a spatial perspective, we calculated both the cumulative estimated occurrence of at-risk species (separately for each cell in a raster covering the extent of the eleven western states) and average risk among species present in a cell. We did this separately for the A and B group species, and we restricted analyses to only species with higher risk values by subsetting to the upper 75th quantile of risk values separately for each list (A and B). Within those higher-risk groups, we converted each species range map from a spatial polygon to a raster layer where values within the range were set to 1 and values outside the range to 0. We summed these values across all rasters to produce a new raster of cumulative estimated species occurrence (also referred to simply as "cumulative occurrence"). To calculate mean risk for each cell, we divided the cumulative risk index raster by the cumulative occurrence raster.

For the evolutionary perspective, we used the phylogeny from Zhang et al. (2019) for all 845 butterfly species from the United States and Canada. Briefly, this tree was based on 756 universal single-copy orthologs we identified from 36 reference genomes using `OrthoMCL` (Li et al. 2003). Sequences of these orthologs were aligned using both local (BLAST [Altschul et al. 1997]) and global (MAFFT [Katoh et al. 2002]) alignment methods, and only positions that were consistently aligned by both methods were used. Sequences of non-reference species were derived by mapping the Illumina reads to the exon sequences of the reference species and performing reference-guided assembly. Multiple sequence alignments (MSA) of different

480 orthologs were concatenated to a single MSA. This MSA was partitioned by codon position and
481 used to build a tree by `IQ-TREE` (version 1.6.12) (Nguyen et al. 2015) with the most suited
482 evolutionary model automatically found by `IQ-TREE`.

483 The phylogeny was imported as a time-calibrated .tre file into R and pruned to our focal
484 western butterflies (the combined A and B group lists). The package `ggtree` (Yu et al. 2017)
485 was used to plot a phylogeny with tips labeled by risk categories assigned based on the quantiles
486 of the risk distributions separately for the A and B group species. Specifically, species in the
487 upper 90th quantile were labeled as "high risk," species between the 75th and 90th quantiles
488 were labeled as "medium risk", and species below the 75th were "low risk." Finally, the
489 phylosig function from `phytools` (Revell 2012) was used to calculate lambda and K (with
490 1000 simulations for the permutation test) as measures of phylogenetic signal for the continuous
491 risk index across all species, which in this context is informative with respect to the extent to
492 which closely related species share similar levels of risk.

493

494 **RESULTS**

495 We calculated an index of risk for 396 species, which includes two groups: 184 species in the A
496 group with extensive monitoring data, and 212 species in the B group without observational data
497 (or without enough to be used in our primary population models). The B group species tend to
498 have smaller geographic ranges (Figure S5), which in part explains their reduced presence (just
499 by geographic chance) in monitoring programs, but the two groups differ in other ways. The B
500 group species have slightly lower exposure to development (Figure S5) and moderately higher
501 exposure to climate change (Figure S5). The higher climate change exposure is explained in part

by the greater presence of more southern species in the B group, as seen by latitudinal midpoints (Figure S5) and qualitative characterization of range (Figure S5).

For the A group species, we modeled historical and projected population trajectories using different sources of observational data. Consistent with previous work with NABA data, our new model with shared (across-species) observation heterogeneity found a majority of species (71%) with annual growth rates below replacement (Figure S6). We used those estimated annual growth rates and the most recent year of observed counts to simulate 50 years into the future. The median fraction of extant locations (or probability of local persistence) per species at 50 years was 0.60, and that fraction was positively related to historical population growth rates (Figure S6). Results from analyses of Shapiro data also find a majority of species with downward trends through time of varying magnitude (84.5% of species have negative year coefficients).

Our risk index and ranking was based on a combination of evidence from the NABA and Shapiro datasets, but note that the A group species are shown in Figure 2 with risk information associated with the other seven variables (geographic range, exposure to development, etc.), even though the actual ranking of the A group is based solely on the observational data. We present the information in this way because we acknowledge the imperfect geographic coverage of monitoring programs and the inherent uncertainty in population models. Thus, the reader or conservation practitioner can easily see if two species with similar risk values in the A group (based on NABA and Shapiro) potentially have similar risk based on other variables like range size.

Without observational data, the ranking of B group species required a partitioning of weights among the other lines of information. To partly inform that process, we used the A group species to estimate the effects of other variables on risk index (based on NABA and Shapiro

525 data). The model explained a relatively small proportion of variance in the risk index (Table S1),
526 but did demonstrate that smaller wingspans (99% probability of effect) and lower range-wide
527 precipitation (98% probability of effect) are associated with risk for the A group species. In
528 addition, we also suspected climate change would be important based on our previous work with
529 western butterflies (Forister et al. 2021, Halsch et al. 2021). This is especially true given the
530 large presence of B group species with ranges in the desert southwest (Figure S5h), a region
531 heavily impacted by warming and drying trends. We adopted the following weighting scheme to
532 calculate a single risk value for species in the B group: 20% precipitation, 20% wingspan, 20%
533 climate change, 10% development, 10% range size, 10% voltinism, and 10% host range;
534 correlations among the seven variables as well as the two observational variables (for the A
535 group) are shown in Figure S7. As a comparison to that scheme, we also ranked the B group
536 species with equal weights (14.3%) among the seven variables; the resulting risk values were
537 correlated at $r = 0.90$ ($t = 29.32$, df = 210, $P < 0.001$) with the values from the primary scheme.
538 With a third weighting scheme based on 50% from each of average range-wide precipitation and
539 wingspan (the two variables identified as most predictive of risk by analysis of the A group), the
540 correlation with the main scheme was $r = 0.57$ ($t = 10.16$, df = 210, $P < 0.001$).

541 The top fifty species with the highest risk values from each of the A and B groups are
542 shown in Figure 2 (the other species with lower risk values are in Figures S8, S9 and S10). For
543 the highest-ranked A group species, agreement between the two monitoring schemes is apparent
544 with large "risk circles" in both the NABA and Shapiro columns (Figure 3a). Time series plots
545 for two of those top species are shown in Figure 3 (*Vanessa annabella*) and Figure 4 (*Euchloe*
546 *ausonides*); in Figure 5, neutral or upward trajectories can be seen for *Poanes melane*, the
547 species with the lowest risk index among the A group species (Figure S10). Similar plots for all

other A group species are available through an online tool (see supplementary material). The rankings for the A group species are shown with 85% credible intervals (Figure 2a), which are broad; this uncertainty reflects the high inter-annual variability inherent to the time series data being modeled (from both NABA and Shapiro) and should be kept in mind when interpreting the position of species on the A group list.

Finally, we examined the distribution of the species-level risk index geographically and phylogenetically, for which we divided the species into low, medium and high risk categories, based on composite risk values below the 75th quantile, between the 75th and 90th quantiles, and above the 90th, respectively. For the A group species, average forecast 50-year occupancy (based on NABA data) was 33.7% of populations extant (standard deviation = 12.5%) for the high risk species, 47.7% occupancy (sd = 11.0%) for the medium risk species, and 66.0% (sd = 13.2%) for the low risk species. Considering the species with medium and high risk index values (above the 75th quantile of risk values) for the A group, the spread of average risk across the 11 western states is only partially associated with expected numbers of the most at-risk species (Figure 6a and 6c). For example, average risk is high in the northern Central Valley of California and in the northwestern region of Oregon (Figure 6a), while the cumulative occurrence of at-risk species is lower in those areas (Figure 6b). Similarly, the number of at-risk species (cumulative occurrence) is high in the Sierra Nevada, but average risk is lower. The distributions of risk for the B group species highlight the bias of that group towards the most southern areas, with high average risk along the southern California coast (Figure 6c) and a concentration of at-risk species along the border between Mexico and New Mexico (Figure 6d).

The phylogenetic picture of risk shows multiple clusters of at-risk species, and some lineages with notably lower risk, like much of the Nymphalidae (Figure 8). The families sharing

571 the disproportionate amount of risk are the Lycaenidae (with 17% of species in the high risk
572 category, above the 90th quantile of risk) and the Hesperiidae (with 14% of species at high risk);
573 these are followed by the Riodinidae (with 13% of species at high risk, albeit based on a small
574 sample size from a family represented by only 8 species) and the Pieridae (with 12% of species
575 at high risk). The percentages of high risk species in the Papilionidae and Nymphalidae are just
576 8% and 2%, respectively (Figure 7). Tests of phylogenetic inertia are consistent with the
577 observation of phylogenetically clustered risk (Pagel's $\lambda = 0.38$, $P < 0.001$; Blomberg's $K =$
578 0.049, $P = 0.001$ based on 1k randomizations), which is evident not only at the family level, but
579 also at lower taxonomic levels, including (among others) within the genera *Lycaena*, *Agathymus*,
580 and *Eurema* (Figure 7).
581

582 **DISCUSSION**

583 Our goal has been to organize and analyze heterogenous data sources in a way that allows
584 conservation biologists to identify the butterflies in the 11 western US states that are most likely
585 to suffer serious reductions in range or population size in coming years. It has not been our
586 objective in this paper to document butterfly declines or to identify traits that make insects more
587 or less sensitive to population stressors, as these topics have been addressed elsewhere for North
588 America (Schultz et al. 2019, Wepprich et al. 2019, Forister et al. 2021), the Neotropics (Janzen
589 and Hallwachs 2019, Salcido et al. 2020), and numerous other parts of the world (Nakamura
590 2011, Fox 2013, Wagner 2019). We hope that our work on species prioritization advances the
591 issue for conservation practitioners using mixed data types, uneven spatial coverage and
592 uncertainty in historical trends. Although some parts of the world (notably countries in western

593 Europe) have dense coverage with standardized monitoring, prioritization in most of the world
594 will involve some mix of monitoring and trait-based inference.

595 The western states have been our region of study, rather than the entire US, because the
596 impacts of climate change are severe and distinct in this arid region (Gonzalez et al. 2018), and
597 the butterfly fauna is similarly shaped by a unique topography and climatic history (Shapiro
598 1996, Hawkins 2010). As a consequence of expansive areas with low human population density,
599 about half of the butterfly species in the region are not included in the monitoring datasets used
600 here, yet we have brought together information on the entire fauna (with the exception of a few
601 species with rare occurrences, mostly strays across the US-Mexico border). Because of this, our
602 study has an apples-and-oranges structure (species with and without monitoring data) that
603 extends to the interpretation of the risk index values and engenders certain ironies. Chief among
604 the ironies of our work is the fact that we rank B group species in part by certain variables
605 (geographic range, exposure to climate change, etc.) that are not strongly associated with
606 declines in the species for which we have historical records (the A group). In other words,
607 considering Figure 2, the A group species near the top of the list do not necessarily have the
608 smallest ranges, and the same can be said of other variables. Even for the two variables
609 (wingspan and average precipitation) which do predict risk in the A group, the variance
610 explained is low (Table S1) yet we still emphasize these variables in ranking the B group
611 species. We discuss these apparently counterintuitive decisions below, and then discuss
612 phylogenetic and geographic hotspots of risk. Finally, we end with a consideration of individual
613 taxa most deserving of attention given available evidence.

614 Among the complexities of variables potentially associated with risk, an understanding of
615 geographic range starts by noting that the A group species have broader geographic ranges

616 (Figure S5a), which is part of the reason they are present at enough NABA sites to be included in
617 our core population model. Thus the fact that many of the most severely declining species are
618 widespread (e.g., *Vanessa annabella* in all 11 states) does not diminish the logic of prioritizing B
619 group species based in part on small range size, which is a well-known determinant of risk
620 (Staude et al. 2020). Similarly, the effects of voltinism and ecological host specialization are
621 relatively straightforward: everything else being equal, we expect a species with multiple
622 generations per year and an ability to utilize many hosts to be more resilient (to any number of
623 stressors) than another species without those traits (Eskildsen et al. 2015).

624 The interpretation of other variables is less straightforward, chief among them being
625 exposure to climate change. Previous work with western butterflies has identified warming and
626 drying conditions as stressors, based in particular on analyses of geographic variation among
627 study sites in climate change effects and changes in aggregate butterfly density (Forister et al.
628 2021). At the species level (rather than the level of individual study sites), the same signal is not
629 as apparent in the present study for the A group species (in other words, the species towards the
630 top of the A group list do not have particularly high exposures to climate change). This is
631 because most of these species have large enough ranges that their exposure to climate change
632 (when quantified across the entire range) includes areas with both more and less severe warming
633 and drying that tend to cancel each other out at the scale of broadly-distributed species.
634 However, the B group species have smaller and more southern ranges (Figure S5), which is the
635 part of the west most impacted by climate change (Gonzalez et al. 2018). Thus, we believe
636 exposure to climate change is well justified as a contributing factor to risk specifically for these
637 species for which we lack monitoring data.

638 Exposure to development (urban, suburban and agricultural lands) requires similarly
639 careful interpretation. This is chiefly because the data most well suited to understanding the
640 effects of habitat destruction on insects will rarely be collected: places that have already been
641 developed will not be monitored, and existing monitoring efforts will often be located in more
642 pristine locations even when relatively proximate to human habitation (Wagner et al. 2021). The
643 Shapiro dataset is an exception, as it encompasses a severe land use gradient from the
644 agricultural and urban Central Valley to the undeveloped high elevations of the Sierra Nevada.
645 From that program, we know that land conversion and contamination (with pesticides) have
646 effects of similar magnitude at low elevations (Forister et al. 2016). Though similar information
647 does not exist across the west, we included exposure to development in our rankings here for the
648 B group species for the simple reason that common sense suggests that a range that encompasses
649 more development is likely to experience increasing fragmentation and contamination in coming
650 years relative to a species with less exposure.

651 Geographic projections of risk for B group species emphasize the southern areas of the
652 west (Figure 6), but also point to specific hotpots of average risk that include the southern
653 California coast. Like A group species in the Central Valley of California, that coastal region has
654 a low cumulative occurrence of B group species, but on average the species that are there in the
655 vicinity of the Los Angeles basin score high for our risk factors. Arizona and southwestern New
656 Mexico have a high concentration of B group species with high risk factors, thus this area should
657 be prioritized for future monitoring efforts. For A group species, the Sierra Nevada Mountains
658 (especially the northern Sierra), the Colorado Plateau and the southern Rocky Mountains are
659 hotspots of declining species (Figure 6). These same places have been recently identified as

660 hotspots of imperiled species in analyses that included plants, vertebrates, freshwater
661 invertebrates and some terrestrial insects (Hamilton et al. 2022).

662 Phylogenetically, risk values are strongly clustered within and among families, with
663 notable concentrations in the Lycaenidae and Hesperiidae, with the latter in part due to both
664 species with small southern ranges (B group species) and species in monitoring programs with
665 observed declines. The phylogenetic clustering of risk suggests that currently unknown or
666 unmeasured variables could in the future improve our ability to model interspecific variation in
667 populations trajectories and extinction risk. On the other hand, the non-random distribution of
668 risk among species and lineages suggests that species loss might itself be clustered, leading to
669 shifts in the function and composition of assemblages (Sol et al. 2017). At present, we can say
670 that of the high-risk category species (with risk index values above the 90th quantile), 46% are
671 Hesperiidae. The family Nymphalidae has the lowest concentration of at-risk species, although
672 one of the most notably-declining species is in this family. Despite being large and dispersive
673 and able to use a number of exotic plants as larval hosts, *Vanessa annabella* is becoming hard to
674 find across locations that include urban centers, high mountains, and southern deserts (Figure 3).

675 Although *V. annabella* is deservedly at the top of the risk list (Figures 2 and 3), we stress
676 the uncertainty in the actual risk values that we have generated and we do not place much weight
677 on the exact position of species on that list. In other words, we believe that the top species in the
678 A group are indeed in historical declines that will likely continue in coming years, but the fact
679 that one species is in the 4th position vs the 10th or even the 25th position on the list is not
680 necessarily important. Small differences in, for example, the projected 50-year probability of
681 population persistence affect the positions for those top species which have mostly similar risk
682 values (and broadly overlapping credible intervals). This is why we conservatively suggest that

683 all of the top 50 species in the A group (Figure 2) deserve closer scrutiny and in some cases
684 likely deserve protection. The fact that rankings should be treated as approximate is also why we
685 have presented other lines of information (geographic range, host specialization, etc.) for the A
686 group, even though the risk index ranking is based solely on the observational data (NABA and
687 Shapiro) for those species. For example, *Pontia protodice* and *Lycaena xanthoides* have nearly
688 identical risk indices, but the latter (*L. xanthoides*) is univoltine with a smaller geographic range,
689 greater exposure to development and a more specialized diet (Figure 2); these are all factors that
690 could be considered by conservation biologists and ecologists interested in declining insects.
691 With respect to current protections, only two of the species that we have studied have status at
692 the federal level: one of the A group species (the monarch butterfly, *Danaus plexippus*) is
693 currently a candidate for protection under the US Endangered Species Act (ESA), and one of the
694 B group species, *Lycaena hermes*, is currently listed as threatened.

695 Our presentation of the top 50 species in the A group (Figure 2) includes sample sizes
696 (for NABA and Shapiro datasets) which should also be considered when judging the evidence
697 for risk. For example, the 2nd and 3rd species on the A group list (Figure 2) are represented by
698 data from 3 or fewer sites for the NABA and Shapiro datasets. The small samples for those
699 species are reflected in broad intervals around the risk values, and it can be noted that other
700 species in the top 10 for the A list are known to be in decline based on evidence from two to
701 three times as many sites (e.g., *Pholisora catullus*, *Atalopedes campestris*, and *Euchloe*
702 *ausonides*). The number of sites for individual species is a reflection not just of information
703 available for analysis, but it should be remembered that risk associated with the NABA data
704 derives from a multi-species population viability analysis. In that analysis, species with fewer
705 sites are more likely by chance to have lower occupancy in forecasts than species known from a

706 greater number of sites. This is both a methodological feature of stochastic simulations but also
707 reflects a biological reality in that more widespread species are known from a greater number of
708 NABA sites (thus geographic range is indirectly involved in the contribution that the NABA
709 analyses make to our estimate of risk).

710 Yet another important aspect of sample size involves A group species not represented in
711 both of the observational datasets; for these species, we used median interpolation. In other
712 words, when calculating the risk index for a species present in, for example, the Shapiro dataset
713 but not NABA, we assigned a 50-year projection value based on the median across all other
714 species represented in the NABA dataset. For the present effort, we consider this to be at least a
715 relatively simple assumption, although we acknowledge that future analyses could use more
716 sophisticated interpolation perhaps including information from closely related species. The
717 phylogenetic signal observed here suggests that genetic relatedness could be a tool for dealing
718 with uncertainty and missing data in conservation ranking.

719 The weight of missing data and uncertainty of course becomes greater when we turn to
720 the top 50 species in the B group (Figure 2) for which monitoring data is either absent or
721 insufficient for robust models. Not only is robust observational data lacking, but so many of the
722 B group species are similar in having small ranges in hot and dry parts of the region that the
723 overall spread of risk values is smaller than for the A group. Thus, rankings in the top 50 for the
724 B group should be treated as approximate. For example, *Strymon avalona* is restricted entirely to
725 Catalina Island (less than 200 square kilometers) off the coast of southern California. The partly
726 wild nature of the island gives the species a low development score and the area happens to be
727 characterized by only moderate departure from climatic baseline. Thus *S. avalona* ranks towards
728 the bottom of the top 50 for the B group (Figure 2), even though that small geographic range of

course puts it at high risk of stochastic loss. Similarly, many of the B group species below the top 50 have negative annual trends (indicated by red lambda symbols to the right of the panel in Figures S8 - S10), albeit based on very few NABA sites (which is why we have shown those results but did not use them in the calculation of the B group risk index). In general we hope that the data organized here for the B group species is an inspiration for greater monitoring of these taxa with small ranges in regions vulnerable to threats that include ongoing climate change and the loss of natural disturbance regimes (Haddad 2018).

CAVEATS & CONCLUSIONS

Our synthesis of status and trends for a diverse fauna faced many challenges. Chief among these is the fact that even for species that are relatively well represented in monitoring schemes, the information is still clustered around areas of human population density. Thus, broad ranges (e.g., Figure 3) and more narrow ranges (e.g., Figure 5) alike are not particularly well sampled in terms of the spread of monitored locations in space. We hope that these results inspire greater investment in state-level monitoring programs, as already exist in some parts of the US (Taron and Ries 2015, Wepprich et al. 2019), and which could eventually fill data gaps and lead to a national understanding of butterfly status on par with countries in Europe. Coming years should also see the development of new models that can take advantage of mixed data types including those reported from crowd-sourced platforms (e.g, Strebel et al. 2022). Our estimation of risk has not included exposure to pesticides, which is available at the county level for California, but not for other states in region, although we know that it is an important stressor (Forister et al. 2016).

Another important issue that we acknowledge is that our estimates of exposure to development and climate change are restricted to the portions of geographic ranges found in the

752 11 western states. This was mainly motivated by our focus on the unique exposure of the region
753 to warming and drying trends, but it is of course the case that wide ranging species might have
754 other parts of their range subject to divergent pressures. Future analyses of risk could quantify
755 heterogeneity of stressors at continental scales. In the meantime, it is for these reasons that we
756 have included our qualitative range labels (N, S, E, and W) with our rankings (Figure 2), which
757 the reader can use to focus as desired on species for which the majority of their range is
758 encompassed within the focal, western region.

759 The traditional focus for butterfly conservation in the United States has been at the
760 taxonomic level of subspecies, which is partly a consequence of the fact that population
761 segments cannot be listed for invertebrates (thus leaving subspecies as the next unit below full
762 species that can be protected). Thus, we acknowledge that our results fall partly outside of the
763 traditional scope of conservation work for butterflies in the United States. It is, however, entirely
764 likely that compounding population losses across the wild spaces of the region have pushed
765 many full species to the point where range-wide research and conservation attention are
766 warranted. A notable example of this is recent effort focused on conservation of the monarch
767 butterfly, *Danaus plexippus* (Pelton et al. 2019), which is indeed in our list of the 50 most at-risk
768 species (Figure 3), but a number of species are higher on the list and are equally deserving of
769 attention. Research in coming years might also profitably focus on species that appear to be
770 relatively stable. One example (*Poanes melane*) is shown in Figure 5, and others can be found
771 toward the end of the ranked list of species in Figure S10, including *Ochlodes agricola, Papilio*
772 *rutulus*, and *Limenitis lorquini*. We hesitate to use the common metaphor of winners and losers.
773 That implies that the game is over, when of course the Anthropocene is underway. Nevertheless,
774 the diversity of ecologies, morphologies and geographic ranges among the stable or increasing

species (Figure S10) suggests that much could be learned about combinations of traits potentially associated with resilience. It is our hope that the results presented here are a framework that will facilitate such work in coming decades, acknowledging the many assumptions that have been made along the way to synthesize diverse data and organize species by composite risk scores.

ACKNOWLEDGEMENTS

MLF thanks the National Science Foundation (DEB-2114793), and CAH was supported by a National Institute of Food and Agriculture fellowship (NEVW-2021-09427). EMG, KLB, and JPJ were supported by the Modelscape Consortium with funding from NSF (OIA-2019528). Thanks to the Plant Insect Group at UNR for much thoughtful feedback, and Lee Dyer in particular for various key ideas, as well as Sarina Jepsen who provided important feedback on subspecies risk. We thank Texas State University for the use of the LEAP computing cluster, and thanks also to authors of our previous analysis of western butterflies (Forister et al. 2021) without which the current paper would not have gotten off the ground.

CONFLICT OF INTEREST

The authors declare no conflict of interest.

AUTHOR CONTRIBUTIONS

MLF conceived the project and the overall organization of data and the presentation of results. TVR wrote the Bayesian population models for the NABA data and contributed to the design of analyses. EMG contributed to numerous components, especially the analysis of spatial data. KJB organized information on subspecies. CAH, CFC, KLB, and TB contributed to component

analyses and assisted with data collation or organization. JZ, QC, and NVG generated the phylogeny which was analyzed here by JPJ. JG manages the collection of NABA data and contributed the expert-derived range outlines. AMS has collected the vast majority of the Shapiro transect data (with a few recent years of collection contributed in part by MLF and CAH). All authors contributed to interpretation of results and writing of the manuscript.

DATA AVAILABILITY STATEMENT

NABA data analyzed for this paper are available at 10.5281/zenodo.4460647; Shapiro transect data and all code will be archived on figshare.com upon acceptance for publication; code used is not novel to this project (relevant functions and packages are cited).

REFERENCES

Abatzoglou, J. T., S. Z. Dobrowski, and S. A. Parks. 2020. Multivariate climate departures have outpaced univariate changes across global lands. Scientific Reports 10:1–9.

Abatzoglou, J. T., S. Z. Dobrowski, S. A. Parks, and K. C. Hegewisch. 2018. TerraClimate, a high-resolution global dataset of monthly climate and climatic water balance from 1958–2015. Scientific Data 5:170191.

Altschul, S. F., T. L. Madden, A. A. Schäffer, J. Zhang, Z. Zhang, W. Miller, and D. J. Lipman. 1997. Gapped BLAST and PSI-BLAST: a new generation of protein database search programs. Nucleic acids research 25:3389–3402.

Benton, T. G. 2003. Understanding the ecology of extinction: are we close to the critical threshold? Annales Zoologici Fennici 40:71–80.

Bonelli, S., L. P. Casacci, F. Barbero, C. Cerrato, L. Dapporto, V. Sbordoni, S. Scalercio, A.

821 Zilli, A. Battistoni, and C. Teofili. 2018. The first red list of Italian butterflies. Insect
822 Conservation and Diversity 11:506–521.
823 Brook, B. W., N. S. Sodhi, and C. J. A. Bradshaw. 2008. Synergies among extinction drivers
824 under global change. Trends in Ecology & Evolution 23:453–460.
825 Cardoso, P., P. S. Barton, K. Birkhofer, F. Chichorro, C. Deacon, T. Fartmann, C. S. Fukushima,
826 R. Gaigher, J. C. Habel, and C. A. Hallmann. 2020. Scientists' warning to humanity on
827 insect extinctions. Biological Conservation 242:108426.
828 Cardoso, P., T. L. Erwin, P. A. V Borges, and T. R. New. 2011. The seven impediments in
829 invertebrate conservation and how to overcome them. Biological Conservation 144:2647–
830 2655.
831 Casner, K., M. L. Forister, K. Ram, and A. M. Shapiro. 2014a. The utility of repeated presence-
832 absence data as a surrogate for counts: a case study using butterflies. Ecological
833 Applications 18:13–27.
834 Casner, K. L., M. L. Forister, J. M. O'Brien, J. H. Thorne, D. P. Waetjen, and A. M. Shapiro.
835 2014b. Loss of agricultural land and a changing climate contribute to decline of an urban
836 butterfly fauna. Conservation Biology 28:773–782.
837 Collins, T. J. 2007. ImageJ for microscopy. Biotechniques 43:S25–S30.
838 Diniz-Filho, J. A. F., P. De Marco Jr, and B. A. Hawkins. 2010. Defying the curse of ignorance:
839 perspectives in insect macroecology and conservation biogeography. Insect Conservation
840 and Diversity 3:172–179.
841 Dirzo, R., H. S. Young, M. Galetti, G. Ceballos, N. J. B. Isaac, and B. Collen. 2014. Defaunation
842 in the Anthropocene. Science 345:401–406.
843 Edge, D. A., and S. Mecenero. 2015. Butterfly conservation in southern Africa. Journal of Insect

Conservation 19:325–339.

Eisenhauer, N., A. Bonn, and C. A Guerra. 2019. Recognizing the quiet extinction of invertebrates. Nature Communications 10:1–3.

Eskildsen, A., L. G. Carvalheiro, W. D. Kissling, J. C. Biesmeijer, O. Schweiger, and T. T. Høye. 2015. Ecological specialization matters: long-term trends in butterfly species richness and assemblage composition depend on multiple functional traits. Diversity and Distributions 21:792–802.

Farber, O., and R. Kadmon. 2003. Assessment of alternative approaches for bioclimatic modeling with special emphasis on the Mahalanobis distance. Ecological Modelling 160:115–130.

Forister, M. L., B. Cousens, J. G. Harrison, K. Anderson, J. H. Thorne, D. Waetjen, C. C. Nice, M. De Parsia, M. L. Hladik, and R. Meese. 2016. Increasing neonicotinoid use and the declining butterfly fauna of lowland California. Biology Letters 12:20160475.

Forister, M. L., J. A. Fordyce, C. C. Nice, J. H. Thorne, D. P. Waetjen, and A. M. Shapiro. 2018. Impacts of a millennium drought on butterfly faunal dynamics. Climate Change Responses 5:3.

Forister, M. L., C. A. Halsch, C. C. Nice, J. A. Fordyce, T. E. Dilts, J. C. Oliver, K. L. Prudic, A. M. Shapiro, J. K. Wilson, and J. Glassberg. 2021. Fewer butterflies seen by community scientists across the warming and drying landscapes of the American West. Science 371:1042–1045.

Forister, M. L., A. C. McCall, N. J. Sanders, J. A. Fordyce, J. H. Thorne, J. O'Brien, D. P. Waetjen, and A. M. Shapiro. 2010. Compounded effects of climate change and habitat alteration shift patterns of butterfly diversity. Proceedings of the National Academy of

867 Sciences of the United States of America 107:2088–2092.
868 Forister, M. L., and A. M. Shapiro. 2003. Climatic trends and advancing spring flight of
869 butterflies in lowland California. Global Change Biology 9:1130–1135.
870 Fox, R. 2013. The decline of moths in Great Britain: a review of possible causes. Insect
871 Conservation and Diversity 6:5–19.
872 Fox, R., M. S. Warren, T. M. Brereton, D. B. Roy, and A. Robinson. 2011. A new Red List of
873 British butterflies. Insect Conservation and Diversity 4:159–172.
874 Geyle, H. M., M. F. Braby, M. Andren, E. P. Beaver, P. Bell, C. Byrne, M. Castles, F. Douglas,
875 R. V Glatz, and B. Haywood. 2021. Butterflies on the brink: identifying the Australian
876 butterflies (Lepidoptera) most at risk of extinction. Austral Entomology 60:98–110.
877 Glassberg, J. 2017. A Swift guide to butterflies of North America. 2nd edition. Princeton
878 University Press.
879 Glassberg, J. 2018. A Swift guide to butterflies of Mexico and Central America. 2nd edition.
880 Princeton University Press.
881 Gonzalez, P., F. Wang, M. Notaro, D. J. Vimont, and J. W. Williams. 2018. Disproportionate
882 magnitude of climate change in United States national parks. Environmental Research
883 Letters 13:104001.
884 Goulson, D. 2019. The insect apocalypse, and why it matters. Current Biology 29:R967–R971.
885 Haddad, N. M. 2018. Resurrection and resilience of the rarest butterflies. PLoS Biology
886 16:e2003488.
887 Hallmann, C. A., M. Sorg, E. Jongejans, H. Siepel, N. Hofland, H. Schwan, W. Stenmans, A.
888 Müller, H. Sumser, T. Hörren, and others. 2017. More than 75 percent decline over 27 years
889 in total flying insect biomass in protected areas. PlOS ONE 12:e0185809.

Halsch, C. A., A. M. Shapiro, J. A. Fordyce, C. C. Nice, J. H. Thorne, D. P. Waetjen, and M. L. Forister. 2021. Insects and recent climate change. Proceedings of the National Academy of Sciences:10.1073/pnas.2002543117.

Hamilton, H., R. L. Smyth, B. E. Young, T. G. Howard, C. Tracey, S. Breyer, D. R. Cameron, A. Chazal, A. K. Conley, and C. Frye. 2022. Increasing taxonomic diversity and spatial resolution clarifies opportunities for protecting imperiled species in the US. Ecological Applications:e2534.

Hawkins, B. A. 2010. Multiregional comparison of the ecological and phylogenetic structure of butterfly species richness gradients. Journal of Biogeography 37:647–656.

Hijmans, R. J., J. van Etten, M. Mattiuzzi, M. Sumner, J. A. Greenberg, O. P. Lamingueiro, A. Bevan, E. B. Racine, and A. Shortridge. 2021. raster: Geographic Data Analysis and Modeling, Version 2.9-23, R package.

Hughes, J. B., G. C. Daily, and P. R. Ehrlich. 2000. Conservation of insect diversity: a habitat approach. Conservation Biology 14:1788–1797.

Jamwal, P. S., M. Di Febbraro, M. L. Carranza, M. Savage, and A. Loy. 2021. Global change on the roof of the world: Vulnerability of Himalayan otter species to land use and climate alterations. Diversity and Distributions.

Janzen, D. H., and W. Hallwachs. 2019. Perspective: Where might be many tropical insects? Biological Conservation 233:102–108.

Katoh, K., K. Misawa, K. Kuma, and T. Miyata. 2002. MAFFT: a novel method for rapid multiple sequence alignment based on fast Fourier transform. Nucleic Acids Research 30:3059–3066.

Kellner, K. 2017. R Package ‘jagsUI’: a wrapper around ‘rjags’ to streamline ‘JAGS’Analyses,

913 v.1.4.9.
914 van Klink, R., D. E. Bowler, K. B. Gongalsky, A. B. Swengel, A. Gentile, and J. M. Chase.
915 2020. Meta-analysis reveals declines in terrestrial but increases in freshwater insect
916 abundances. Science 368:417–420.
917 Li, L., C. J. Stoeckert, and D. S. Roos. 2003. OrthoMCL: identification of ortholog groups for
918 eukaryotic genomes. Genome Research 13:2178–2189.
919 Maes, D., W. Vanreusel, I. Jacobs, K. Berwaerts, and H. Van Dyck. 2012. Applying IUCN Red
920 List criteria at a small regional level: a test case with butterflies in Flanders (north
921 Belgium). Biological Conservation 145:258–266.
922 McLaughlin, J. F., J. J. Hellmann, C. L. Boggs, and P. R. Ehrlich. 2002. Climate change hastens
923 population extinctions. Proceedings of the National Academy of Sciences of the United
924 States of America 99:6070–6074.
925 NABA. 2018. Checklist of North American Butterflies Occurring North of Mexico - Edition 2.4.
926 Naeem, S., R. Chazdon, J. E. Duffy, C. Prager, and B. Worm. 2016. Biodiversity and human
927 well-being: an essential link for sustainable development. Proceedings of the Royal Society
928 B: Biological Sciences 283:20162091.
929 Nakamura, Y. 2011. Conservation of butterflies in Japan: status, actions and strategy. Journal of
930 Insect Conservation 15:5–22.
931 New, T. R., R. M. Pyle, J. A. Thomas, C. D. Thomas, and P. C. Hammond. 1995. Butterfly
932 Conservation Management. Annual Review of Entomology 40:57–83.
933 Nguyen, L.-T., H. A. Schmidt, A. Von Haeseler, and B. Q. Minh. 2015. IQ-TREE: a fast and
934 effective stochastic algorithm for estimating maximum-likelihood phylogenies. Molecular
935 Biology and Evolution 32:268–274.

Nice, C. C., M. L. Forister, Z. Gompert, J. A. Fordyce, and A. M. Shapiro. 2014. A hierarchical perspective on the diversity of butterfly species' responses to weather in the Sierra Nevada Mountains. Ecology 95:2155–2168.

Opler, P. A. 1999. A field guide to western butterflies. Houghton Mifflin Harcourt.

Pelham, J. P. 2022. A catalogue of the butterflies of the United States and Canada.

Pelton, E. M., C. B. Schultz, S. J. Jepsen, S. H. Black, and E. E. Crone. 2019. Western monarch population plummets: status, probable causes, and recommended conservation actions. Frontiers in Ecology and Evolution 7:258.

RCoreTeam. 2020. R: A language and environment for statistical computing R Foundation for Statistical Computing, Vienna, Austria. URL https://www.R-project.org/.

Revell, L. J. 2012. phytools: an R package for phylogenetic comparative biology (and other things). Methods in Ecology and Evolution:217–223.

Riecke, T. V, D. Gibson, M. Kéry, and M. Schaub. 2021. Sharing detection heterogeneity information among species in community models of occupancy and abundance can strengthen inference. Ecology and evolution 11:18125–18135.

Salcido, D. M., M. L. Forister, H. G. Lopez, and L. A. Dyer. 2020. Ecosystem services at risk from declining taxonomic and interaction diversity in a tropical forest. Scientific Reports 10:1–10.

Samways, M. J. 2007. Insect conservation: a synthetic management approach. Annu. Rev. Entomol. 52:465–487.

Schultz, C. B., N. M. Haddad, E. H. Henry, and E. E. Crone. 2019. Movement and demography of at-risk butterflies: building blocks for conservation. Annual Review of Entomology 64:167–184.

Scott, J. A. 1986. The butterflies of North America. Stanford University Press, Stanford, California.

Sekar, S. 2012. A meta-analysis of the traits affecting dispersal ability in butterflies: can wingspan be used as a proxy? Journal of Animal Ecology 81:174–184.

Sen, P. K. 1968. Estimates of the regression coefficient based on Kendall's tau. Journal of the American Statistical Association 63:1379–1389.

Shapiro, A. M. 1996. Status of butterflies. Pages 743–757 Sierra Nevada Ecosystem Project: Final Report to Congress Vol. II. Center for Water and Wildland Resources, University of California, Davis, Davis, California.

Shapiro, A. M. 2022. Art Shapiro's Butterfly Site https://butterfly.ucdavis.edu/.

Sol, D., I. Bartomeus, C. González-Lagos, and S. Pavoine. 2017. Urbanisation and the loss of phylogenetic diversity in birds. Ecology Letters 20:721–729.

Staude, I. R., L. M. Navarro, and H. M. Pereira. 2020. Range size predicts the risk of local extinction from habitat loss. Global Ecology and Biogeography 29:16–25.

Strebel, N., M. Kéry, J. Guélat, and T. Sattler. 2022. Spatiotemporal modelling of abundance from multiple data sources in an integrated spatial distribution model. Journal of Biogeography 49:563–575.

van Swaay, C., D. Maes, S. Collins, M. L. Munguira, M. Šašić, J. Settele, R. Verovnik, M. Warren, M. Wiemers, and I. Wynhoff. 2011. Applying IUCN criteria to invertebrates: How red is the Red List of European butterflies? Biological Conservation 144:470–478.

Taron, D., and L. Ries. 2015. Butterfly monitoring for conservation. Pages 35–57 Butterfly Conservation in North America. Springer.

Theil, H. 1950. A rank-invariant method of linear and polynomial regression analysis.

Indagationes Mathematicae 12:173.

Turvey, S. T., and J. J. Crees. 2019. Extinction in the Anthropocene. Current Biology 29:R982–R986.

USDA. 2020. National Agricultural Statistics Service Cropland Data Layer. Published crop-specific data layer. https://nassgeodata.gmu.edu/CropScape/.

Wagner, D. L. 2019. Insect declines in the Anthropocene. Annual Review of Entomology 65.

Wagner, D. L., E. M. Grames, M. L. Forister, M. R. Berenbaum, and D. Stopak. 2021. Insect decline in the Anthropocene: Death by a thousand cuts. Proceedings of the National Academy of Sciences 118:e2023989118.

Wepprich, T., J. R. Adrion, L. Ries, J. Wiedmann, and N. M. Haddad. 2019. Butterfly abundance declines over 20 years of systematic monitoring in Ohio, USA. PLOS ONE 14:e0216270.

Wilson, E. O. 1987. The little things that run the world (the importance and conservation of invertebrates). Conservation Biology 1:344–346.

Yu, G., D. K. Smith, H. Zhu, Y. Guan, and T. T. Lam. 2017. ggtree: an R package for visualization and annotation of phylogenetic trees with their covariates and other associated data. Methods in Ecology and Evolution 8:28–36.

Zhang, J., Q. Cong, J. Shen, P. A. Opler, and N. V Grishin. 2019. Genomics of a complete butterfly continent. BioRxiv:829887.

1001 **Figure legends**

1002

1003 **FIGURE 1** Schematic overview of main inputs, processes and products associated with the
1004 generation of risk index values. As noted in the key, data sources are in brown, analyses (and
1005 other calculations) are in blue boxes, variables (used in the creation of the risk index) are in red,
1006 and the primary products are in green. The central branching path illustrates the division of
1007 species into the A and B groups, with monitoring data contributing to the A group risk
1008 assessment on the left, and other data types contributing to B group assessment on the right. The
1009 9 variables (in red) are identical to the columns in Figure 2, although labelled slightly different
1010 here, especially for the observational variables: "β year" is the year coefficient from analyses of
1011 Shapiro data summarizing change through time, and "P(persistence)" is the probability of
1012 population persistence from 50-year forecasts. Variables on the right ("range area",
1013 "precipitation," etc.) are more self-explanatory. Also note that the expert-derived geographic
1014 ranges contribute to the risk index calculations both directly ("range area" and "voltinism") and
1015 indirectly as indicated with connecting arrows. Finally, the "Risk analysis" process box (towards
1016 the lower left) illustrates the analysis of A group risk that was used to partly inform the
1017 weighting scheme for the B group species.

1018

1019 **FIGURE 2** The top 50 species with the highest risk values in the A group (on the left) and the B
1020 group (on the right). The two panels have some features in common, and some unique elements.
1021 In common they both show the extent to which different variables are associated with higher or
1022 lower risk for each species: a large circle under NABA occupancy, for example, marks a species
1023 that we infer as being at risk because of low forecast occupancy (probability of population

persistence) across currently-extant locations; similarly, a large circle under development indicates a species at risk because of high exposure to developed lands, and a large circle under geographic range indicates corresponding risk associated with a relatively small range. The sizes of the circles were assigned separately within the two lists, A and B group species, and thus indicate relative differences within those lists. Although all variables are shown for comparison, the overall risk ranking for the A group species is based solely on the first two variables (NABA occupancy and Shapiro monitoring, to the left of the vertical gray line), while the ranking for the B group species is based entirely on the other seven variables (see main text for details, and Figure 1). Both panels also have in common the quantitative risk values shown to the right (e.g., the risk index for *Vanessa annabella* in panel A is 0.687); note that the risk values for the A group species include 85% credible intervals (in parentheses), encompassing uncertainty derived from Bayesian analyses of both NABA and Shapiro data. The capital letters (N, S, E and W) running down the left side of each panel are qualitative biogeographical descriptions indicating where the mass of a geographic range lies relative to the western US (N and S indicate species found primarily north and south of the US borders with Canada and Mexico, respectively; W indicates species with the majority of their range in our focal region; and E indicates species found either mostly in the eastern US or with a transcontinental distribution), and the asterisks next to species names flag taxonomic issues (see Table S2). A unique element of the panel on the left is the sample size in parentheses, e.g. "(14,10)" for *Vanessa annabella*, which is the number of locations from which data were included from the NABA and Shapiro datasets, respectively. Finally, on the far right of panel (b), the lambda symbols represent the results of individual time series models run for the species present in the NABA program but without enough sites and years to be included in the main model (and thus not a part of the A list); a blue symbol indicates

a species with an 80% or greater probability of increasing in recent years, while a red symbol indicates an 80% chance of decreasing, and black is neither increasing nor decreasing. The other species (beyond the top 50 highest ranked shown here) are included in Figures S8, S9, and S10.

FIGURE 3 Overview of site-specific trends through time for *Vanessa annabella* at Shapiro sites (on the left) and NABA sites (on the right and along the bottom). Plots for Shapiro sites are shown with decreasing elevation (cooler colors are montane sites) and colored to match the elevational profile of Northern California shown below the map of the western US. The y-axes for Shapiro plots are the fraction of days a species was seen at a site in a year (Shapiro data were truncated at 1984 for analyses, but earlier years are shown here and in Figures 4 and 5). Plots for NABA sites are shown with decreasing latitude (starting with the most northern sites), from the top right to the bottom, with symbols matching the locations shown in the central map. Values shown in NABA plots have been adjusted for variation in sampling effort, and values plotted are total counts of individuals on a natural log scale. Also shown on the central map is the geographic range of *V. annabella* (Glassberg 2017), with the multivoltine portion of the range (closer to the coast) shown as darker gray. Adult and caterpillar images by Camryn Maher, copyright 2022.

FIGURE 4 Overview of site-specific trends through time for *Euchloe ausonides* at Shapiro sites (on the left) and NABA sites (on the right). Plots for Shapiro sites are shown with decreasing elevation (cooler colors are montane sites) and colored to match the elevational profile of Northern California shown below the map of the western US. The y-axes for Shapiro plots are the fraction of days a species was seen at a site in a year. Plots for NABA sites are shown with

decreasing latitude (starting with the most northern sites), with symbols matching the locations shown in the central map. Values shown in NABA plots have been adjusted for variation in sampling effort, and values plotted are total counts of individuals on a natural log scale. The geographic range of *E. ausonides* (Glassberg 2017) is shown as the gray shaded area on the central map. Adult and caterpillar images by Camryn Maher, copyright 2022.

FIGURE 5 Overview of site-specific trends through time for *Poanes melane* at Shapiro sites (on the left) and NABA sites (on the right). Plots for Shapiro sites are shown with decreasing elevation (cooler colors are montane sites) and colored to match the elevational profile of Northern California shown below the map of the western US. The y-axes for Shapiro plots are the fraction of days a species was seen at a site in a year. Plots for NABA sites are shown with decreasing latitude (starting with the most northern sites), with symbols matching the locations shown in the central map and insect. Values shown in NABA plots have been adjusted for variation in sampling effort, and values plotted are total counts of individuals on a natural log scale. The geographic range of *P. melane* is shown as the gray shaded are on the central map. Adult and caterpillar images by Camryn Maher, copyright 2022.

FIGURE 6 The geography of risk for species with values in the upper 75th quantile of risk indices as shown in Figure 2 (i.e., combining "medium" and "high" risk categories treated separately in Figure 7). Panels (a) and (b) show average risk values among those high risk species, separately for the A and B group species, while panels (c) and (d) show cumulative estimated species occurrence, again for the A group and B group species separately.

1093 **FIGURE 7** The phylogenetic distribution of risk, here shown as three categories: high risk
1094 (upper 90th quantile), medium risk (75th to 90th quantiles), and low risk (below the 75th
1095 quantile). Species names in black are the A group species, other are B group. Butterfly images as
1096 follows: (A) *Apodemia mormo* (Riodinidae); (B) *Euphilotes pallescens arenamontana*
1097 (Lycaenidae); (C) *Euchloe ausonides* (Pieridae); (D) *Polites sabuleti* (Hesperiidae); (E) *Adelpha*
1098 *bredowii* (Nymphalidae); (F) *Papilio rutulus* (Papilionidae). Photo credits go to CAH (panels A,
1099 C, E, and F); MLF (panels B and D). Bootstrap support is not shown but the vast majority of
1100 nodes have support above 0.95; see Zhang et al. (2019) for additional details.

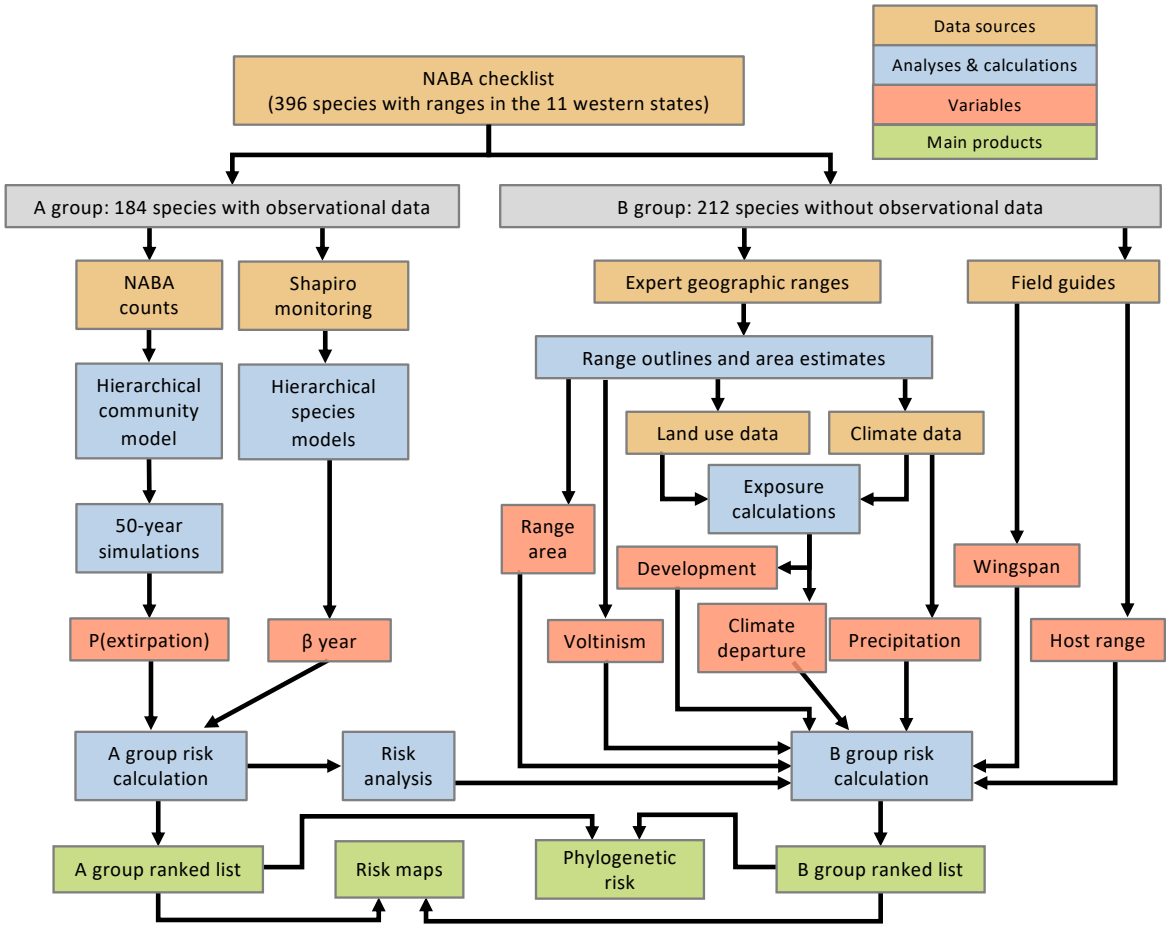
Data sources
Analyses & calculations
Variables
Main products
NABA checklist
(396 species with ranges in the 11 western states)
A group: 184 species with observational data
B group: 212 species without observational data
NABA counts
Shapiro monitoring
Expert geographic ranges
Field guides
Range outlines and area estimates
Hierarchical community model
Hierarchical species models
Land use data
Climate data
Exposure calculations
50-year simulations
Range area
Development
Wingspan
P(extirpation)
β year
Voltinism
Climate departure
Precipitation
Host range
A group risk calculation
Risk analysis
B group risk calculation
A group ranked list
Risk maps
Phylogenetic risk
B group ranked list

Figure 1

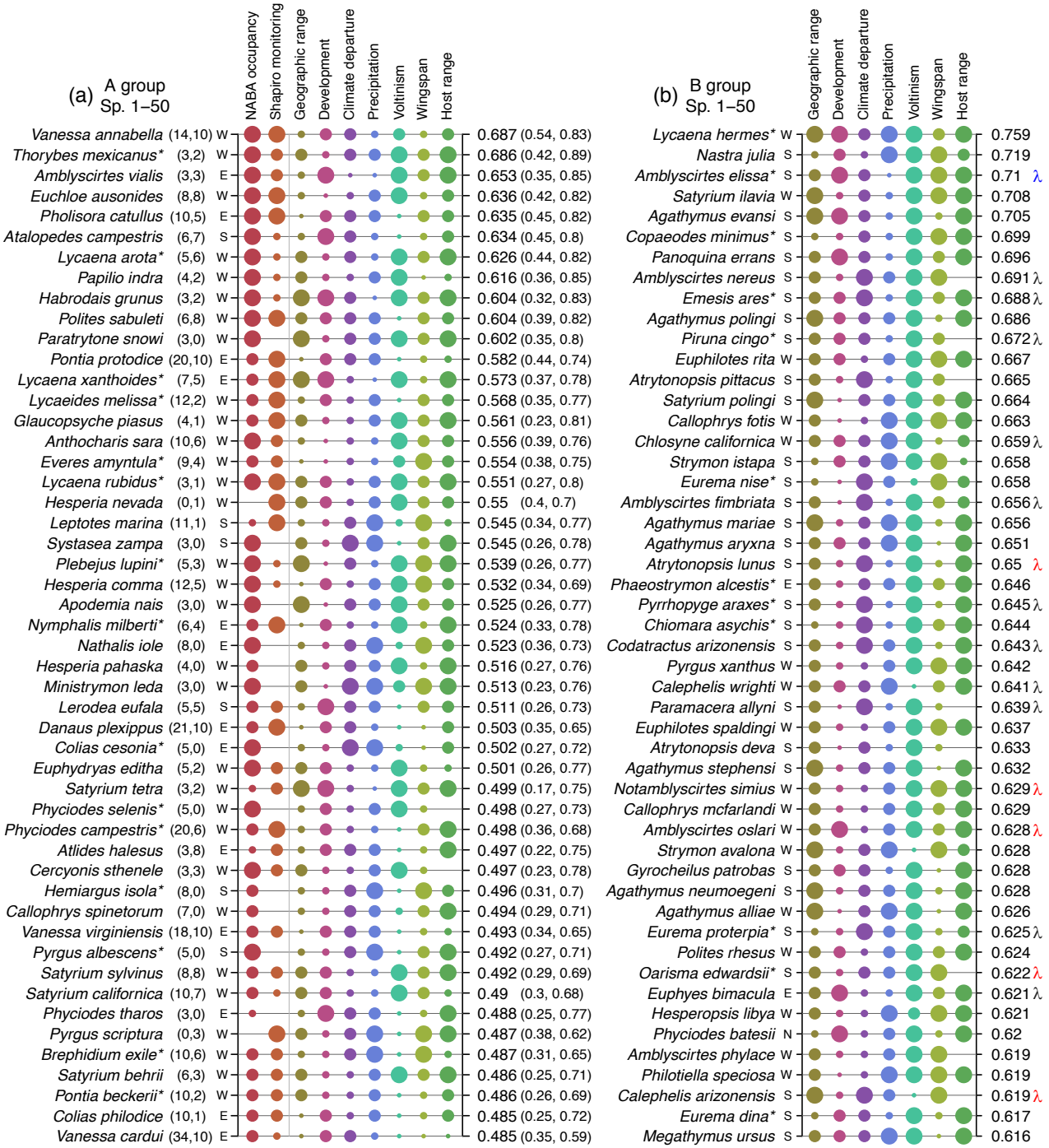
(a) A group Sp. 1–50
NABA occupancy
Shapiro monitoring
Geographic range
Development
Climate departure
Precipitation
Voltinism
Wingspan
Host range
Vanessa annabella (14,10) W 0.687 (0.54, 0.83)
Thorybes mexicanus* (3,2) W 0.686 (0.42, 0.89)
Amblyscirtes vialis (3,3) E 0.653 (0.35, 0.85)
Euchloe ausonides (8,8) W 0.636 (0.42, 0.82)
Pholisora catullus (10,5) E 0.635 (0.45, 0.82)
Atalopedes campestris (6,7) S 0.634 (0.45, 0.8)
Lycaena arota* (5,6) W 0.626 (0.44, 0.82)
Papilio indra (4,2) W 0.616 (0.36, 0.85)
Habrodais grunus (3,2) W 0.604 (0.32, 0.83)
Polites sabuleti (6,8) W 0.604 (0.39, 0.82)
Paratrytone snowi (3,0) W 0.602 (0.35, 0.8)
Pontia protodice (20,10) E 0.582 (0.44, 0.74)
Lycaena xanthoides* (7,5) E 0.573 (0.37, 0.78)
Lycaeides melissa* (12,2) W 0.568 (0.35, 0.77)
Glaucopsyche piasus (4,1) W 0.561 (0.23, 0.81)
Anthocharis sara (10,6) W 0.556 (0.39, 0.76)
Everes amyntula* (9,4) W 0.554 (0.38, 0.75)
Lycaena rubidus* (3,1) W 0.551 (0.27, 0.8)
Hesperia nevada (0,1) W 0.55 (0.4, 0.7)
Leptotes marina (11,1) S 0.545 (0.34, 0.77)
Systasea zampa (3,0) S 0.545 (0.26, 0.78)
Plebejus lupini* (5,3) W 0.539 (0.26, 0.77)
Hesperia comma (12,5) W 0.532 (0.34, 0.69)
Apodemia nais (3,0) W 0.525 (0.26, 0.77)
Nymphalis milberti* (6,4) E 0.524 (0.33, 0.78)
Nathalis iole (8,0) E 0.523 (0.36, 0.73)
Hesperia pahaska (4,0) W 0.516 (0.27, 0.76)
Ministrymon leda (3,0) W 0.513 (0.23, 0.76)
Lerodea eufala (5,5) S 0.511 (0.26, 0.73)
Danaus plexippus (21,10) E 0.503 (0.35, 0.65)
Colias cesonia* (5,0) E 0.502 (0.27, 0.72)
Euphydryas editha (5,2) W 0.501 (0.26, 0.77)
Satyrium tetra (3,2) W 0.499 (0.17, 0.75)
Phyciodes selenis* (5,0) W 0.498 (0.27, 0.73)
Phyciodes campestris* (20,6) W 0.498 (0.36, 0.68)
Atlides halesus (3,8) E 0.497 (0.22, 0.75)
Cercyonis sthenele (3,3) W 0.497 (0.23, 0.78)
Hemiargus isola* (8,0) S 0.496 (0.31, 0.7)
Callophrys spinetorum (7,0) W 0.494 (0.29, 0.71)
Vanessa virginiensis (18,10) E 0.493 (0.34, 0.65)
Pyrgus albescens* (5,0) S 0.492 (0.27, 0.71)
Satyrium sylvinus (8,8) W 0.492 (0.29, 0.69)
Satyrium californica (10,7) W 0.49 (0.3, 0.68)
Phyciodes tharos (3,0) E 0.488 (0.25, 0.77)
Pyrgus scriptura (0,3) W 0.487 (0.38, 0.62)
Brephidium exile* (10,6) W 0.487 (0.31, 0.65)
Satyrium behrii (6,3) W 0.486 (0.25, 0.71)
Pontia beckerii* (10,2) W 0.486 (0.26, 0.69)
Colias philodice (10,1) E 0.485 (0.25, 0.72)
Vanessa cardui (34,10) E 0.485 (0.35, 0.59)
(b) B group Sp. 1–50
Geographic range
Development
Climate departure
Precipitation
Voltinism
Wingspan
Host range
Lycaena hermes* W 0.759
Nastra julia S 0.719
Amblyscirtes elissa* S 0.71 λ
Satyrium ilavia W 0.708
Agathymus evansi S 0.705
Copaeodes minimus* S 0.699
Panoquina errans S 0.696
Amblyscirtes nereus S 0.691 λ
Emesis ares* S 0.688 λ
Agathymus polingi S 0.686
Piruna cingo* S 0.672 λ
Euphilotes rita W 0.667
Atrytonopsis pittacus S 0.665
Satyrium polingi S 0.664
Callophrys fotis W 0.663
Chlosyne californica W 0.659 λ
Strymon istapa S 0.658
Eurema nise* S 0.658
Amblyscirtes fimbriata S 0.656 λ
Agathymus mariae S 0.656
Agathymus aryxna S 0.651
Atrytonopsis lunus S 0.65 λ
Phaeostrymon alcestis* E 0.646
Pyrrhopyge araxes* S 0.645 λ
Chiomara asychis* S 0.644
Codatractus arizonensis S 0.643 λ
Pyrgus xanthus W 0.642
Calephelis wrighti W 0.641 λ
Paramacera allyni S 0.639 λ
Euphilotes spaldingi W 0.637
Atrytonopsis deva S 0.633
Agathymus stephensi S 0.632
Notamblyscirtes simius W 0.629 λ
Callophrys mcfarlandi W 0.629
Amblyscirtes oslari W 0.628 λ
Strymon avalona W 0.628
Gyrocheilus patrobas S 0.628
Agathymus neumoegeni S 0.628
Agathymus alliae W 0.626
Eurema proterpia* S 0.625 λ
Polites rhesus W 0.624
Oarisma edwardsii* S 0.622 λ
Euphyes bimacula E 0.621 λ
Hesperopsis libya W 0.621
Phyciodes batesii N 0.62
Amblyscirtes phylace W 0.619
Philotiella speciosa W 0.619
Calephelis arizonensis S 0.619 λ
Eurema dina* S 0.617
Megathymus ursus S 0.616

Figure 2

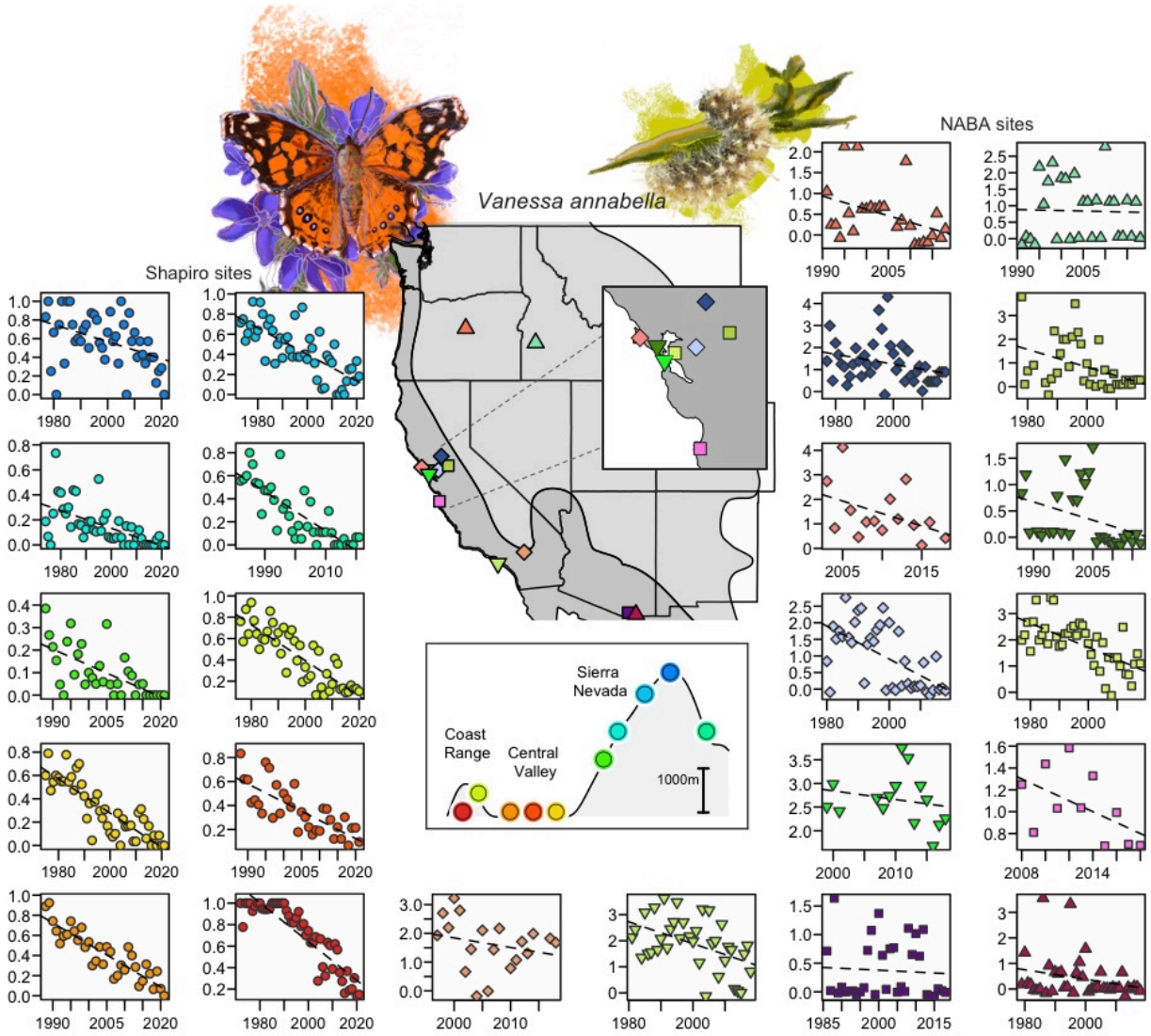
Vanessa annabella
Shapiro sites
NABA sites
Sierra Nevada
Coast Range
Central Valley
1000m

Figure 3

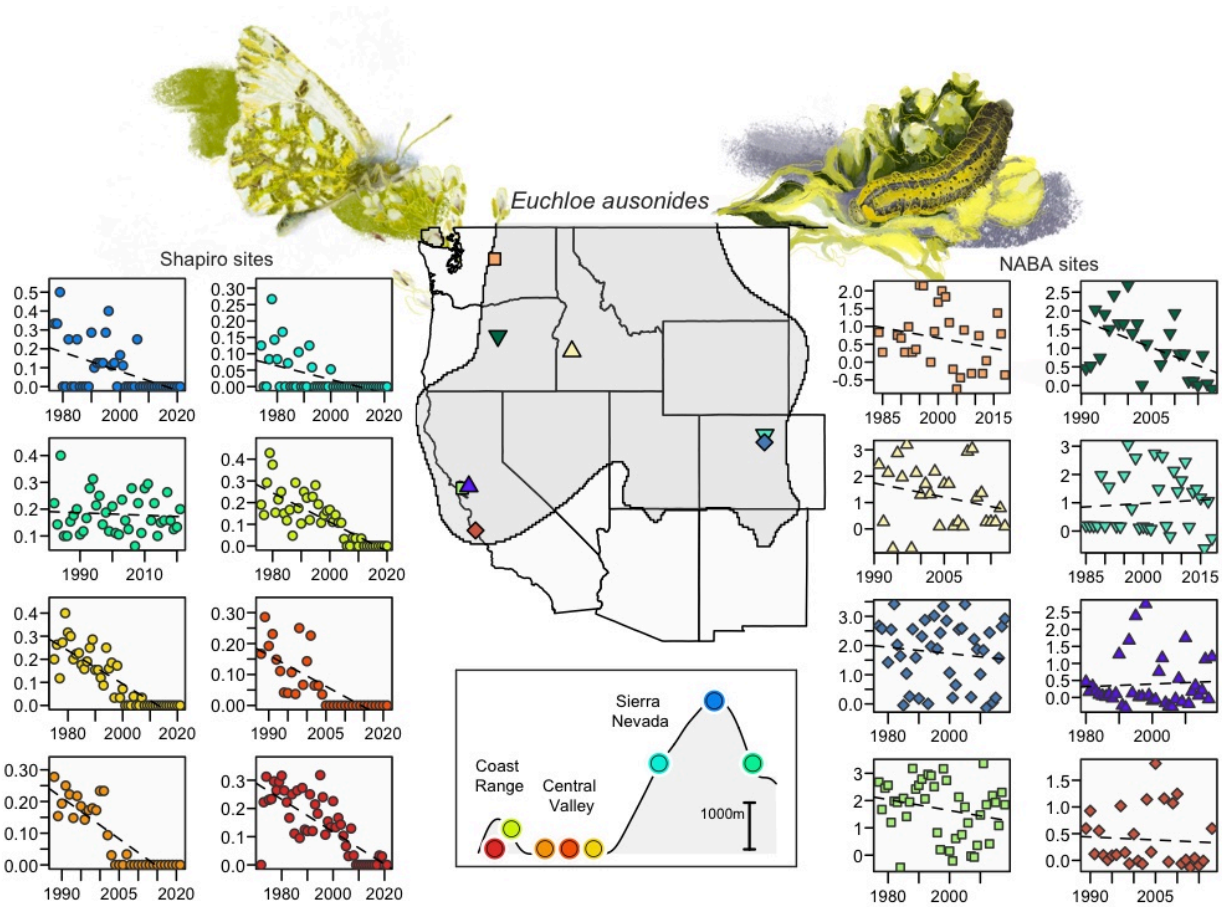
Euchloe ausonides
Shapiro sites
NABA sites
Coast Range
Central Valley
Sierra Nevada
1000m

Figure 4

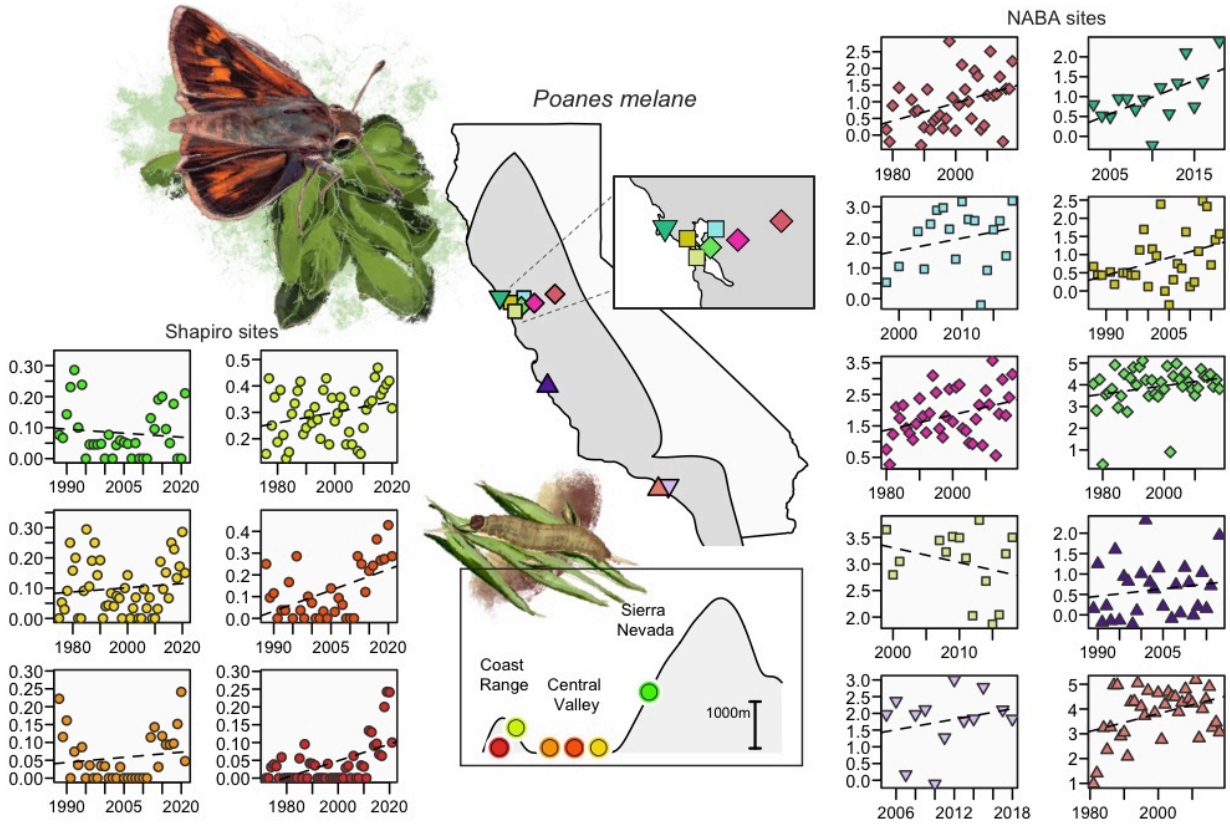
Poanes melane
Shapiro sites
NABA sites
Sierra Nevada
Coast Range
Central Valley
1000m

Figure 5

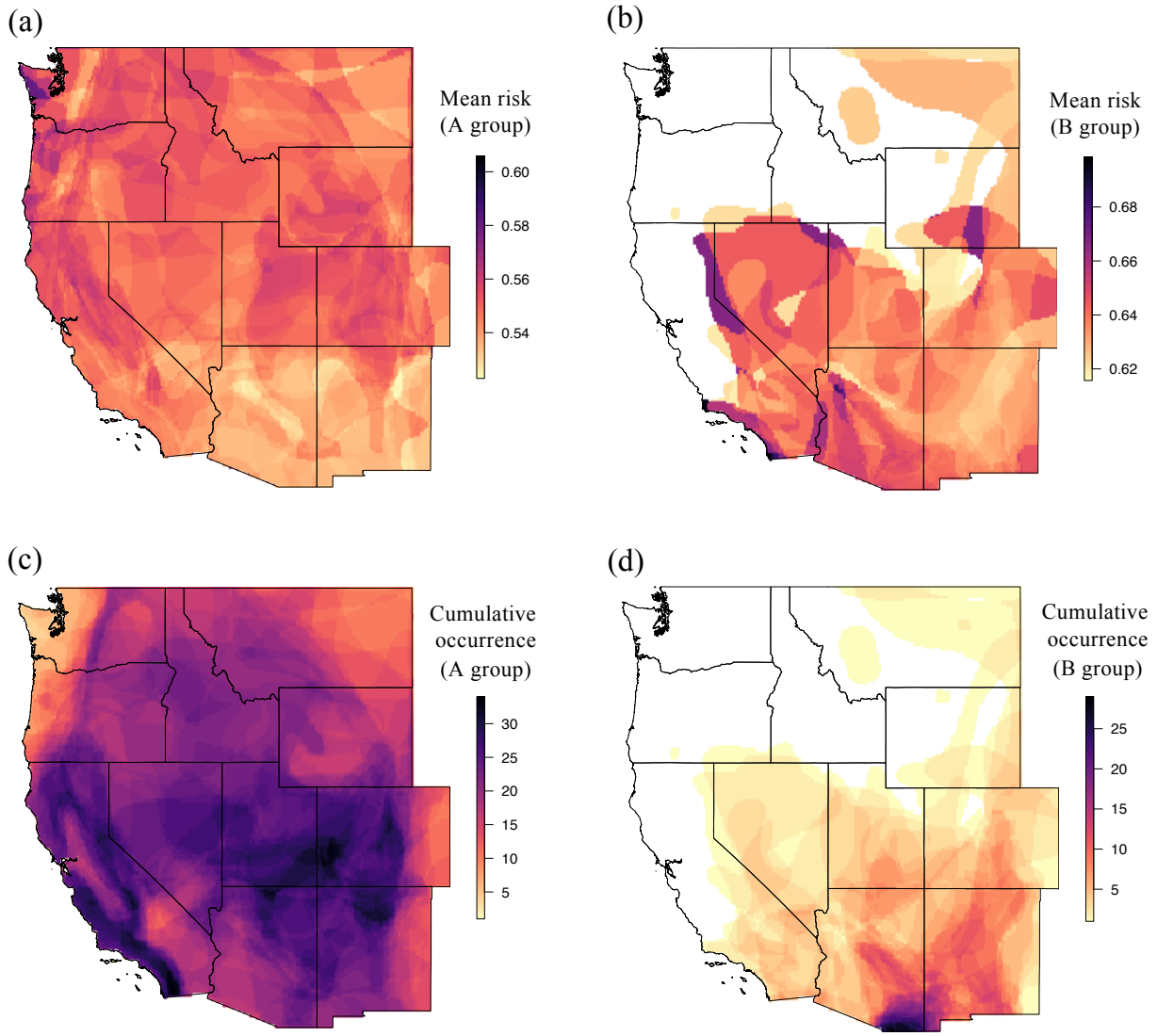
(a)
Mean risk
(A group)
0.60
0.58
0.56
0.54
(b)
Mean risk
(B group)
0.68
0.66
0.64
0.62
(c)
Cumulative
occurrence
(A group)
30
25
20
15
10
5
(d)
Cumulative
occurrence
(B group)
25
20
15
10
5

Figure 6

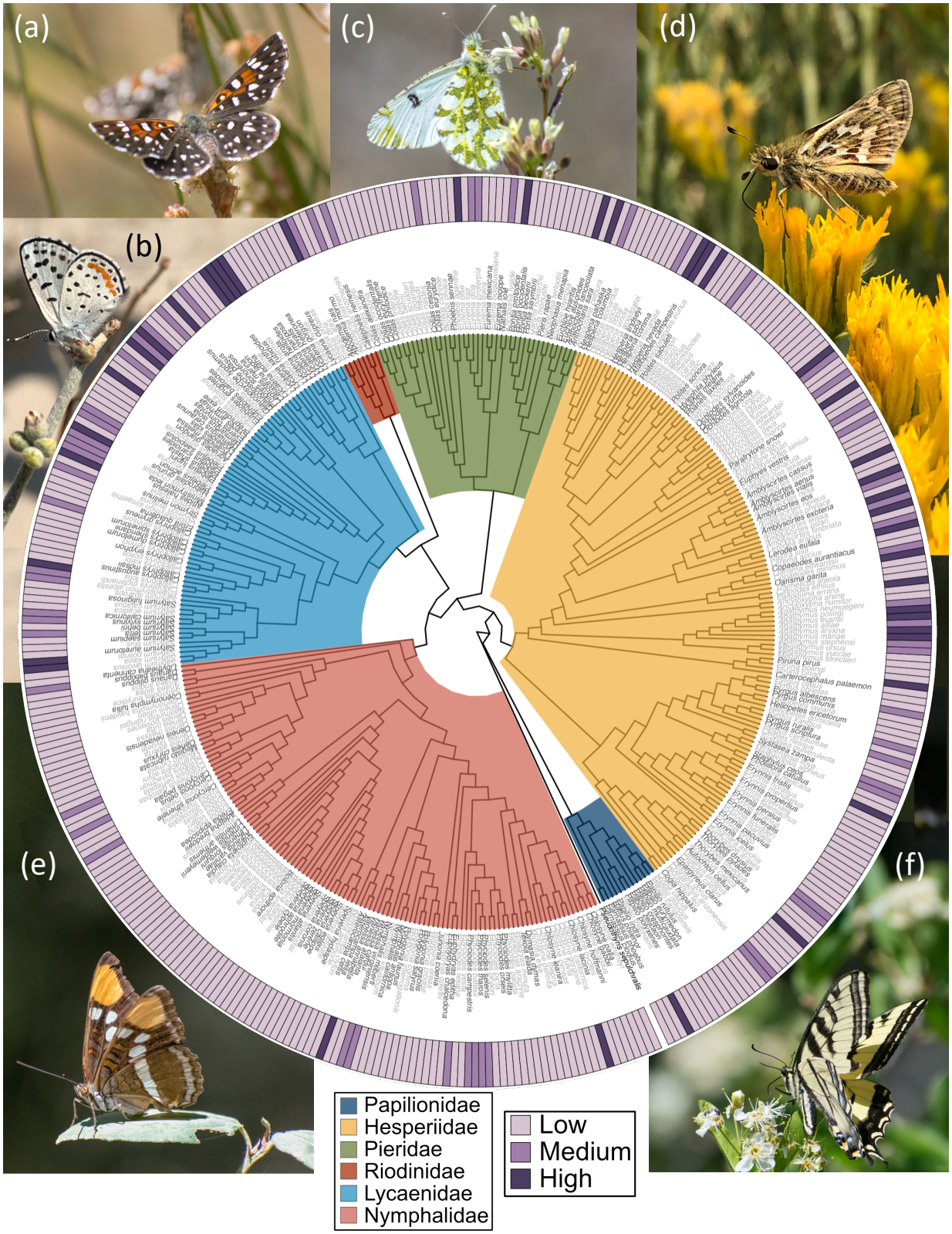
(a)
(b)
(c)
(d)
(e)
(f)
Papilionidae
Hesperiidae
Pieridae
Riodinidae
Lycaenidae
Nymphalidae
Low
Medium
High

Figure 7